



Long-read human genome sequencing and its applications

Glenn A. Logsdon¹, Mitchell R. Vollger¹ and Evan E. Eichler^{1,2}✉

Abstract | Over the past decade, long-read, single-molecule DNA sequencing technologies have emerged as powerful players in genomics. With the ability to generate reads tens to thousands of kilobases in length with an accuracy approaching that of short-read sequencing technologies, these platforms have proven their ability to resolve some of the most challenging regions of the human genome, detect previously inaccessible structural variants and generate some of the first telomere-to-telomere assemblies of whole chromosomes. Long-read sequencing technologies will soon permit the routine assembly of diploid genomes, which will revolutionize genomics by revealing the full spectrum of human genetic variation, resolving some of the missing heritability and leading to the discovery of novel mechanisms of disease.

Next-generation sequencing

A sequencing method in which an entire genome is sequenced from fragmented DNA, producing short (less than 300 bp) sequencing reads at high speed and low cost.

Sequence-by-synthesis

A sequencing technology used primarily by Illumina, in which a DNA polymerase synthesizes a strand of DNA complementary to a template by incorporating a fluorescently labelled deoxynucleoside triphosphate that is imaged to identify the base and then cleaved before the process is repeated to determine the order and identity of each base in the DNA strand.

Studies of genetic variation and the discovery of the mutations underlying human disease are dependent on technological advances in molecular biology and conceptual advances in their application. Among such innovations, changes in sequencing platforms have often been regarded as revolutionary¹. The DNA sequencing technology that has dominated genomics research for the past decade has undoubtedly been the Illumina platform, a short-read, next-generation sequencing platform that leverages a sequence-by-synthesis approach to determine the order of nucleotides in a DNA strand² (FIG. 1a). Illumina's DNA sequencing technology produces highly accurate (greater than 99.9%) sequencing reads, which are inexpensive to generate on a massive scale (TABLE 1). These advantages have driven the ascent of the Illumina platform to become the current gold standard of clinical and research sequencing. Illumina next-generation sequencing has led to innumerable scientific discoveries over the past decade that have enhanced our understanding of evolution, adaptation and disease through the discovery of pathogenic variants, including single-nucleotide variants, copy number variants and insertions or deletions (indels)^{3–8}. Importantly, the technology's throughput has allowed it to serve as an assay for digital readouts to investigate a myriad of biological phenomena, including chromatin accessibility, transcription factor occupancy, gene expression and RNA binding, among many other novel applications².

However, application of short-read technologies to structural variant detection and genome assembly more broadly has revealed a major shortcoming: limited read length. Reads less than 300 bases long, such as those typically produced by Illumina next-generation sequencing, are too short to detect more than 70% of human genome structural variation (that is, variation affecting sequences

longer than 50 bp), with intermediate-size structural variation (less than 2 kb) especially under-represented⁹. Moreover, entire swaths of our genome (more than 15%) remain inaccessible to assembly or variant discovery because of their repeat content or atypical GC content¹⁰. For example, even PCR-free, short-read genomic libraries show up to twofold reductions in sequence coverage when the GC composition exceeds 45%, limiting the ability to discover genetic variation in some of the most functionally important regions of our genome. These inaccessible parts of the genome include centromeres, telomeres and acrocentric genomic regions, where massive arrays of tandem repeats predominate, as well as the 5% of our genome (and associated genes) mapping to large segmental duplications¹¹. Ironically, these regions also experience some of the highest mutation rates, both in the germline and in the soma^{3,12–14}. As a result, some of the most mutable regions of our genome are typically understudied. These limitations have necessitated the development of methods that can resolve these more complex and dynamic regions of the genome.

One solution has been to develop short-read sequencing approaches that reconstruct the sequence of long DNA molecules. Linked-read sequencing^{15–17}, synthetic long-read sequencing^{18,19} and Hi-C²⁰ sequencing are all cost-effective methods that provide long-range information about the location of reads using only Illumina sequencing short reads. For example, Hi-C technology uses a proximity ligation approach to generate a genome-wide library from loci that were originally close to each other in the nucleus, with the majority of loci residing on the same chromosome (FIG. 1b). Hi-C sequencing data can be used to provide long-range information between pairs of loci tens of megabases apart on the same chromosome, which has been shown to link

¹Department of Genome Sciences, University of Washington School of Medicine, Seattle, WA, USA.

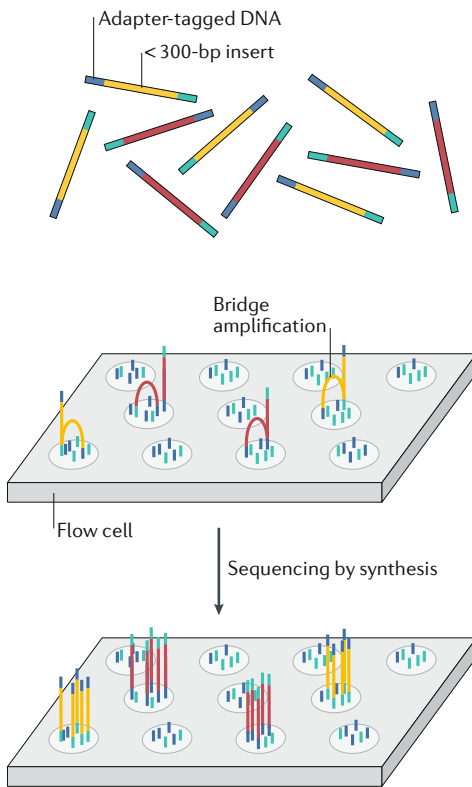
²Howard Hughes Medical Institute, University of Washington, Seattle, WA, USA.

✉e-mail: eee@

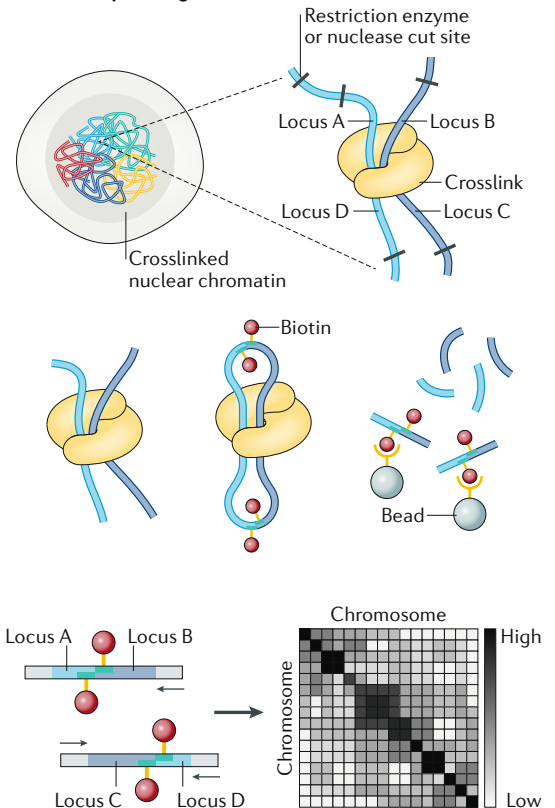
gs.washington.edu

<https://doi.org/10.1038/s41576-020-0236-x>

a Illumina short-read sequencing



b Hi-C sequencing



Single-nucleotide variants
Instances in which a single base within a read or genome differs from the base found at the same position in other individuals or populations.

Copy number variants
Instances in which a sequence of bases within a genome differs in the number of copies among individuals or populations.

Indels
Insertions or deletions of bases in the genome of an organism.

Structural variant
A genetic variant greater than 50 bp in length that includes insertions, deletions, inversions or translocations of DNA segments, and copy number differences.

Segmental duplications
Blocks of DNA that are greater than 1 kb in length, occur at more than one site within a genome and share greater than 90% sequence identity.

Linked-read sequencing
A synthetic long-read DNA sequencing method wherein short-read sequencing is applied to long DNA molecules to 'link' reads together from the same original long molecule.

Long-read sequencing
A sequencing method used by Pacific Biosciences and Oxford Nanopore Technologies, wherein native DNA or RNA molecules are sequenced in real time, often without the need for amplification, producing reads more than 10 kb in length.

Contigs
Continuous (or 'contiguous') sequences of DNA generated by assembling overlapping sequencing reads.

Single-molecule, real-time (SMRT) sequencing
A DNA sequencing method used by Pacific Biosciences wherein the sequence of a single DNA molecule is derived in real time, with no pause after the detection of the bases.

Fig. 1 | Overview of short-read sequencing technologies. a | In short-read sequencing by Illumina technology, DNA fragments (yellow and red) are ligated to adapters (blue and aqua). The adapters contain unique molecular identifiers as well as sequences complementary to the oligonucleotides attached to the surface of a flow cell. Adapter-tagged DNA is loaded onto a flow cell, and the adapters from the modified DNA hybridize to the oligonucleotides that coat the surface of the flow cell. Once the DNA fragments have attached, cluster generation begins, where thousands of copies of each fragment are generated through a process known as bridge amplification. In this process, one strand folds over, and the adapter on the end of the molecule hybridizes to another oligonucleotide in the flow cell. A polymerase incorporates nucleotides to build double-stranded bridges of the DNA molecules, which are subsequently denatured to leave single-stranded DNA fragments tethered to the flow cell. This process is repeated over and over, generating several million dense clusters of double-stranded DNA. After bridge amplification, the reverse DNA strands are cleaved and washed away, leaving only the forward strands. Then, sequencing by synthesis begins, in which fluorescently labelled deoxynucleoside triphosphates are incorporated into the newly synthesized DNA strand at each cycle. After incorporation, a laser excites the fluorophore on the strand, which emits a characteristic fluorescence signal that corresponds to the base. **b** | In Hi-C sequencing, nuclear chromatin is crosslinked with formaldehyde, which covalently bonds protein–DNA complexes in close proximity to each other. Crosslinked chromatin is digested with a restriction enzyme or nuclease, and single-stranded DNA overhangs are filled in and repaired with biotin-linked nucleotides before religating the DNA. Chemical crosslinks are reversed, proteins are degraded and the purified DNA is non-specifically sheared (for example, by sonication). Biotin-labelled DNA is pulled down with streptavidin-conjugated beads and paired-end sequenced to reveal the junctions between two DNA loci (light and dark blue). Because the contact frequency between pairs of loci strongly correlates with distance, the majority of sequenced junctions encompass two loci from the same chromosome. As a result, Hi-C data can be used to provide linkage information between pairs of loci tens of megabases apart on a single chromosome (as shown in the contact map).

contigs in broken genome assemblies²¹, phase haplotypes²², and lead to the discovery of structural variation²³. Although Hi-C outperforms simple short-read sequencing approaches for structural variant detection, the fundamental unit of assembly is still a short read, which greatly limits the ability to both detect and fully assemble structural variant regions, especially in larger repeats. For these applications, the linked-read, synthetic long-read and Hi-C sequencing approaches are generally inferior to strict long-read sequencing approaches⁹.

In this Review, we focus on the two major long-read sequencing technologies, that of Pacific Biosciences

(also known as single-molecule, real-time (SMRT) sequencing, or PacBio sequencing) and that of Oxford Nanopore Technologies (ONT). We compare them with short-read sequencing technologies, such as Illumina sequencing technology, in terms of read accuracy, throughput and cost. Additionally, we discuss the practical applications of these technologies in genomics, transcriptomics and epigenetics and how they are enabling new biological insights. This Review does not provide a detailed assessment of the various software and algorithms related to genome assembly, which is an area of rapid development that has been discussed extensively elsewhere^{24–27}.

SMRTbell

A double-stranded DNA template used in Pacific Biosciences SMRT sequencing wherein both DNA ends are capped with hairpin adapters. A SMRTbell template is topologically circular and structurally linear.

SMRT Cell

A flow cell comprising arrays of zero-mode waveguide nanostructures used during Pacific Biosciences SMRT sequencing.

Zero-mode waveguides

Nanophotonic devices that confine light to a small observation volume and are part of the SMRT Cell used during Pacific Biosciences SMRT sequencing.

Flow cell

A disposable component of short-read and long-read sequencing platforms that houses the chemistry to sequence DNA and/or RNA molecules.

Instead, we focus on future directions, with a specific emphasis on studies of human disease and diversity, while recognizing that these technologies have had a huge impact more broadly across diverse species and phyla.

Long-read sequencing technologies

In contrast to short-read approaches, long-read technologies can generate continuous sequences ranging from 10 kilobases to several megabases in length directly from native DNA, which, along with recent developments in throughput and accuracy, has substantially increased their utility and application^{28,29} (FIG. 2). PacBio and ONT sequencing technologies both produce reads that can readily traverse the most repetitive regions of the human genome, but underlying differences in their chemistry and sequence detection approaches influence their read lengths, base accuracies and throughput.

Pacific Biosciences. PacBio SMRT sequencing technology (FIG. 2a) uses a topologically circular DNA molecule template, known as a SMRTbell, which is composed of a double-stranded DNA insert with single-stranded hairpin adapters on either end. The DNA insert can range in length from one to more than a hundred kilobases, which allows long sequencing reads to be generated. Once the SMRTbell has been assembled, it is bound by a DNA polymerase and loaded onto a SMRT Cell, which contains up to 8 million zero-mode waveguides, for sequencing. During the sequencing reaction, the polymerase processes around the SMRTbell template and incorporates fluorescently labelled deoxynucleoside triphosphates into the nascent strand. After each incorporation, a laser excites the fluorophore, and a camera records the emission. The fluorophore is then cleaved from the nucleotide before the next deoxynucleoside triphosphate is

incorporated. This process is repeated thousands of times to reveal the identity and sequence of each base in the SMRTbell template. PacBio technology typically generates reads tens of kilobases long, which greatly exceeds the read lengths obtained with Illumina sequencing^{30–33}.

Oxford Nanopore Technologies. ONT long-read sequencing technology (FIG. 2b) uses linear DNA molecules rather than circular ones. These linear DNA molecules are typically one to several hundred kilobases in length but can be several megabases long^{34–37}. ONT sequencing begins by first attaching a double-stranded DNA molecule to a sequencing adapter, which is pre-loaded with a motor protein. The DNA mixture is loaded onto a flow cell, which contains hundreds to thousands of nanopores embedded in a synthetic membrane. The motor protein unwinds the double-stranded DNA and, together with an electric current, drives the negatively charged DNA through the pore at a controlled rate. As the DNA translocates through the pore, it causes characteristic disruptions to the current, which are analysed in real time to determine the sequence of the bases in the DNA strand. With ONT sequencing, reads greater than 1 Mb in length have been generated³⁴, with the longest reported read close to 2.3 Mb in length when computationally stitched together from shorter reads³⁷. Together, these achievements have pushed the genomics community into the realm of megabase-sized sequence reads for the first time.

Long-read sequencing data types

Because of new developments in sequencing chemistry and differences in DNA preparation, each of the long-read sequencing technologies can now produce different types of long reads that differ both in their length

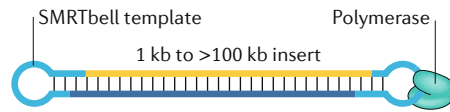
Table 1 | Data type, length, accuracy, throughput and cost across long-read and short-read technologies and platforms

Sequencing technology	Platform	Data type	Read length (kb)		Read accuracy (%)	Throughput per flow cell (Gb)		Estimated cost per Gb (US\$)	Maximum throughput per year (Gb) ^a
			N50	Maximum		Mean	Maximum		
Pacific Biosciences (PacBio)	RS II ^b	CLR	5–15	>60	87–92	0.75–1.5	2	333–933 ^c	4,380
	Sequel	CLR	25–50	>100		5–10	20	98–195 ^d	17,520
	Sequel II	CLR	30–60	>200		50–100	160	13–26 ^e	93,440
		HiFi	10–20	>20	>99	15–30	35	43–86 ^e	10,220
Oxford Nanopore Technologies (ONT)	MinION/ GridION	Long	10–60	>1,000	87–98	2–20	30	50–500 ^f	21,900 (MinION) 109,500 (GridION)
		Ultra-long	100–200	>1,500		0.5–2	2.5	500–2,000 ^f	913 (MinION) 4,563 (GridION)
	PromethION	Long	10–60	>1,000		50–100	180	21–42 ^f	3,153,600
Illumina	NextSeq 550	Single-end	0.075–0.15	0.15	>99.9	16–30	>30	50–63 ^g	>47,782
		Paired-end	0.075–0.15 (×2)	0.15 (×2)		32–120	>120	40–60 ^g	>70,080
	NovaSeq 6000	Single-end	0.05–0.25	0.25		65–3,000	>3,000	10–35 ^h	>1,194,545
		Paired-end	0.05–0.25 (×2)	0.25 (×2)					

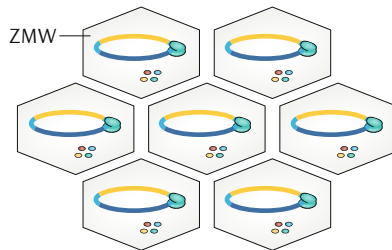
All cost estimates exclude the cost for labour, instrumentation, maintenance and computer resources. CLR, continuous long read; HiFi, high-fidelity read. ^aAssuming continuous, full-capacity sequencing on each instrument. ^bPacBio RS II support will end by 2021. ^cCurrent cost when performing sequencing with a SMRTbell Template Prep Kit 1.0 and SMRT Cell. ^dCurrent cost when performing sequencing with a SMRTbell Express Template Prep Kit 2.0 and SMRT Cell 1M. ^eCurrent cost when performing sequencing with a SMRTbell Express Template Prep Kit 2.0 and SMRT Cell 8M. ^fCurrent cost when performing sequencing with a ligation or rapid sequencing kit and an ONT R9.4.1 or R10.3 flow cell. ^gCurrent cost when performing sequencing with the NextSeq 500/550 mid- or high-output kits v2.5. ^hCurrent cost when performing sequencing with the NovaSeq 6000 SP, S1, S2 or S4 reagent kits.

a PacBio SMRT sequencing

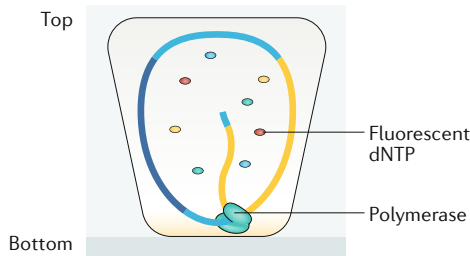
Template topology



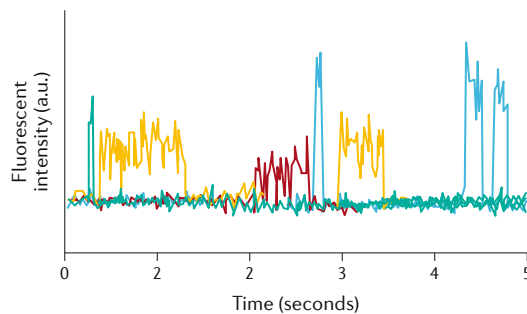
Flow cell (top view)



Single ZMW (cross section)

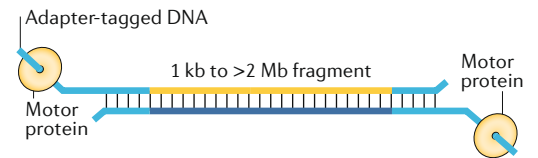


Readout

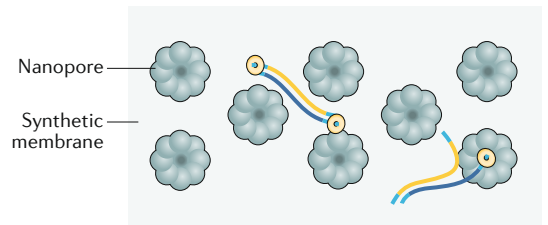


b ONT sequencing

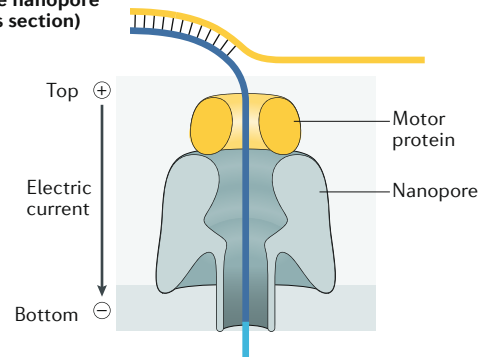
Template topology



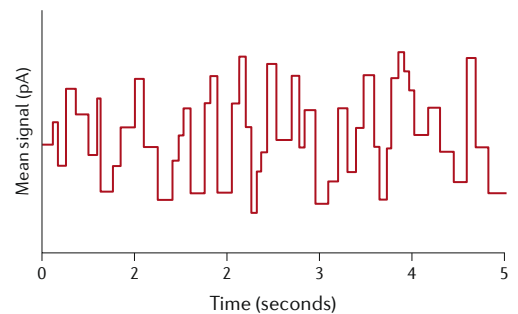
Flow cell (top view)



Single nanopore (cross section)



Readout



Subreads

The sequence derived from a single pass of the DNA polymerase as it processes along the SMRTbell template multiple times during Pacific Biosciences SMRT sequencing. Subreads do not contain any adapter sequences.

Homopolymers

Sequences of consecutive identical bases.

Single-pass

The traversal of a single strand within a SMRTbell template by a DNA polymerase during Pacific Biosciences SMRT sequencing.

Polishing tools

Computational tools that increase genome assembly quality and accuracy. These tools typically compare reads to an assembly to derive a more accurate consensus sequence.

and accuracy (TABLE 1). These diverse data types are, consequently, beginning to be used for specific applications. While long-read base accuracies have been reviewed elsewhere^{38–40}, in the following sections we provide a limited meta-analysis of recently generated long-read datasets to illustrate the relative lengths and base accuracies of each of these data types (FIG. 3; Supplementary Information).

PacBio continuous long reads. Continuous long reads (CLRs) are currently the most common PacBio data type. CLRs are generated by first constructing standard SMRTbell template libraries with DNA inserts greater than 30 kb in length (FIG. 3a). Because of the large insert size in these molecules, the polymerase makes only one or a few passes around the template, generating subreads that typically range from 5 to 60 kb in length

but can be greater than 100 kb long (FIG. 3c; Supplementary Fig. 1; Supplementary Note). Our meta-analysis indicates that CLR subread accuracy is typically 85–92%, with only ~85% of homopolymers at least five bases long accurately called (FIG. 3c,d; Supplementary Fig. 1; Supplementary Note), which is consistent with data reported elsewhere^{31,41–44}. Although the single-pass accuracy of CLRs is low compared with Illumina short-read accuracy (which is greater than 99.9%)⁴⁵, the error mode is remarkably stochastic in nature. As a result, errors can be corrected with polishing tools, such as Quiver⁴⁶ and Arrow, which leverage CLR alignments, along with their underlying raw pulse information, to infer the true sequence of the regions on the basis of sequence consensus. Additional steps are typically used to increase the accuracy and minimize residual indels, such as error correction with Illumina sequencing data

◀ **Fig. 2 | Overview of long-read sequencing technologies. a** | In Pacific Biosciences (PacBio) single-molecule, real-time (SMRT) sequencing, DNA (yellow for forward strand, dark blue for reverse strand) is fragmented and ligated to hairpin adapters (light blue) to form a topologically circular molecule known as a SMRTbell. Once the SMRTbell has been generated, it is bound by a DNA polymerase and loaded onto a SMRT Cell for sequencing. Each SMRT Cell can contain up to 8 million zero-mode waveguides (ZMWs), which are chambers that hold picolitre volumes. Light penetrates the lower 20–30 nm of each well, reducing the detection volume of the well to only 20 zl (10^{-21} l). As the DNA mixture floods the ZMWs, the SMRTbell template and polymerase become immobilized on the bottom of the chamber. Fluorescently labelled deoxynucleoside triphosphates (dNTPs) are added to begin the sequencing reaction. As the polymerase begins to synthesize the new strand of DNA, a fluorescent dNTP is briefly held in the detection volume, and a light pulse from the bottom of the well excites the fluorophore. Unincorporated dNTPs are not typically excited by this light but, in rare cases, can become excited if they diffuse into the excitation volume, thereby contributing to noise and error in PacBio sequencing. The light emitted from the excited fluorophore is detected by a camera, which records the wavelength and relative position of the incorporated base in the nascent strand. The phosphate-linked fluorophore is then cleaved from the nucleotide as part of the natural incorporation of the base into the new strand of DNA and released into the buffer, preventing fluorescent interference during the subsequent light pulse. The DNA sequence is determined by the changing fluorescent emission that is recorded within each ZMW, with a different colour corresponding to each DNA base (for example, green, T; yellow, C; red, G; blue, A). **b** | In Oxford Nanopore Technologies (ONT) sequencing, arbitrarily long DNA (yellow for forward strand, dark blue for reverse strand) is tagged with sequencing adapters (light blue) preloaded with a motor protein on one or both ends. The DNA is combined with tethering proteins and loaded onto the flow cell for sequencing. The flow cell contains thousands of protein nanopores embedded in a synthetic membrane, and the tethering proteins bring the DNA molecules towards these nanopores. Then, the sequencing adapter inserts into the opening of the nanopore, and the motor protein begins to unwind the double-stranded DNA. An electric current is applied, which, in concert with the motor protein, drives the negatively charged DNA through the pore at a rate of about 450 bases per second. As the DNA moves through the pore, it causes characteristic disruptions to the current, generating a readout known as a ‘squiggle’. Changes in current within the pore correspond to a particular *k*-mer (that is, a string of DNA bases of length *k*), which is used to identify the DNA sequence.

Squiggle

A series of voltage shifts that represent overlapping *k*-mers from a DNA molecule as it translocates through a nanopore during Oxford Nanopore Technologies sequencing.

Sequencing coverage

The average number of unique reads that align to, or ‘cover’, a sequence or genome.

Circular consensus sequencing

(CCS). A sequencing mode used by Pacific Biosciences in which a DNA polymerase makes multiple passes around the SMRTbell template, generating noisy subreads that are computationally combined to generate a highly accurate high-fidelity consensus read.

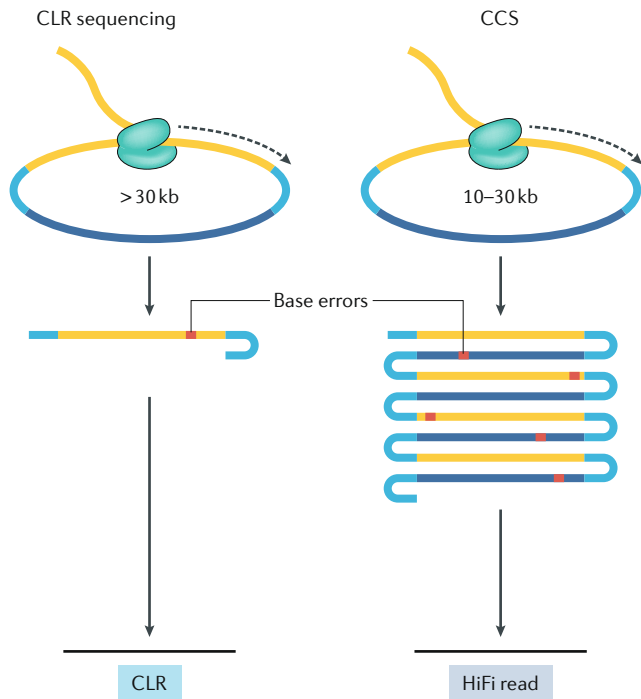
generated from the same individual (for example, with Pilon⁴⁷, Racon⁴⁸, FreeBayes^{49,50} and NextPolish⁵¹); however, error correction with short-read data is limited in repetitive regions (owing to ambiguous mappings) and regions with extreme GC content (owing to reduced coverage arising from biases in short-read sequencing). CLR data can be generated with the RS II, Sequel and Sequel II platforms. Whereas the RS II and Sequel platforms generate only up to 2 Gb and 20 Gb of data per flow cell, respectively, the more recent Sequel II platform with 8 million zero-mode waveguides is capable of generating up to 160 Gb per flow cell in CLR mode (TABLE 1). Thus, it is now possible to obtain greater than 40-fold sequencing coverage of a human genome with only one or two Sequel II flow cells, resulting in more than 99.9% consensus sequence accuracy. Although still more expensive than Illumina sequencing, it is now feasible to contemplate population-scale sequencing of a few hundred samples and family-based sequencing for variant discovery and genome assembly on the basis of Sequel II throughput cost reductions^{9,52} (TABLE 1).

PacBio high-fidelity reads. High-fidelity (HiFi) sequence reads represent the most recent data type to be developed by PacBio. They are the first data type that is both long (greater than 10 kb in length) and highly accurate (greater than 99%). Here, smaller DNA inserts, 10–30 kb in length, are assembled into SMRTbell templates and

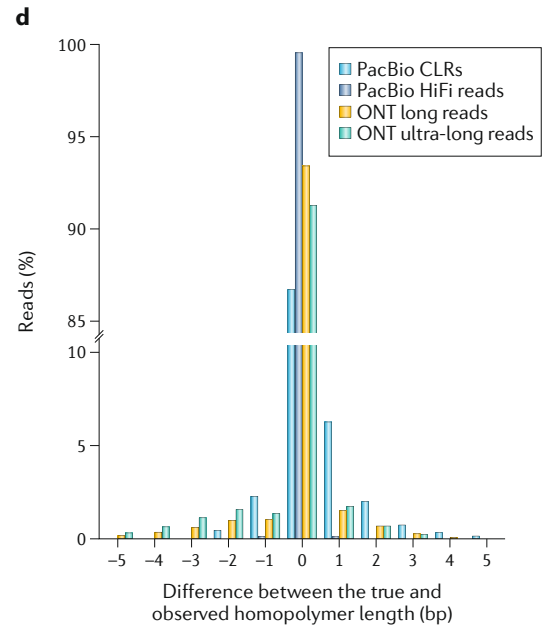
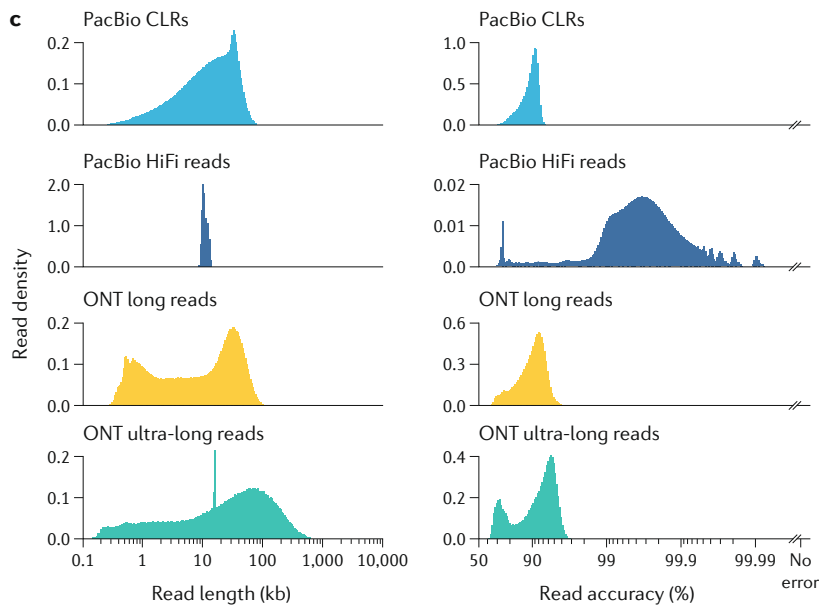
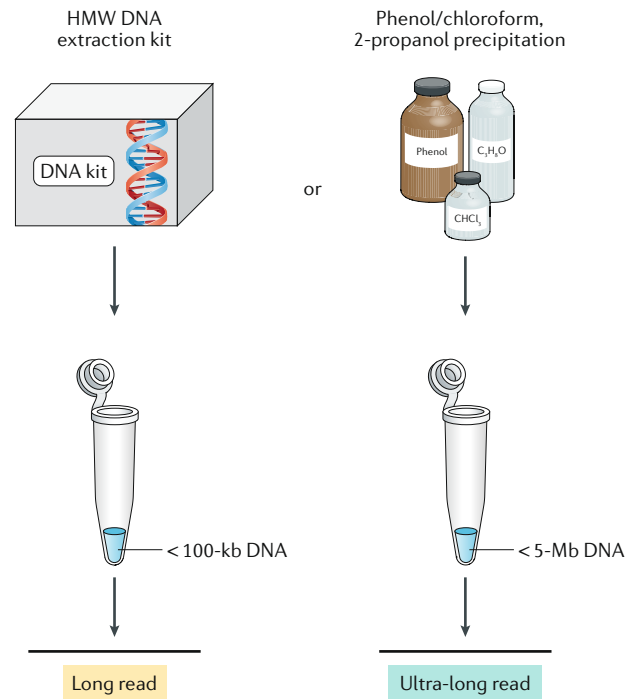
subjected to sequencing via circular consensus sequencing (CCS) (FIG. 3a). Because of the relatively small size of the DNA insert, the polymerase is able to make several passes through the SMRTbell template, resulting in extremely long polymerase reads (read N50 greater than 150 kb in length) that each contain several subreads from both forward and reverse complements of the template. Owing to the increased efficiency of the DNA polymerase during CCS, the subread throughput of the HiFi protocol is increased over that of CLR (more than 200 Gb versus 100 Gb) but requires significantly longer movie times (30 hours) to generate datasets because accuracy is dependent on more passes. Subreads from a single polymerase read are then computationally combined via the CCS algorithm to create a HiFi consensus read, resulting in a total yield of 15–25 Gb of HiFi data from a single SMRT Cell 8M. Thus, approximately three SMRT Cells 8M are required to generate the 25-fold sequencing coverage of a human genome considered sufficient for de novo assembly^{52,53}, equating to approximately two to three times the cost of CLR data (TABLE 1). Each SMRT Cell 8M is run sequentially on the Sequel II system and, therefore, takes several days to generate 25-fold sequencing coverage. Additionally, the process of converting subreads into HiFi reads via the CCS algorithm carries a significant computational investment and can require more than 10,000 CPU hours per SMRT Cell 8M of data^{52,53}. However, recent improvements in the CCS algorithm have reduced this time to less than 2,000 CPU hours per SMRT Cell 8M of data (see [Pacific Biosciences: does speed impact quality and yield?](#)). Typically, the CCS algorithm requires three or four subreads from the same molecule to eliminate the majority of stochastic errors and to achieve the minimum accuracy of 99%⁵³. However, once they have been generated, our meta-analysis indicates that HiFi reads have a median accuracy greater than 99.9%, with over 99.5% of homopolymers at least five bases long accurately resolved, consistent with data reported elsewhere^{53,54} (FIG. 3c,d; Supplementary Fig. 1; Supplementary Note). The high accuracy of PacBio HiFi sequence data has improved variant discovery, reduced the time to assembly and provided access to even more complex regions of repetitive DNA, including the contiguous assembly of some human centromeres^{52,53,55}. More than 50% of the regions previously inaccessible with Illumina short-read sequence data in the GRCh37 human reference genome are now accessible with HiFi reads⁵³. Although HiFi reads are especially useful for cDNA sequencing due to their comparatively high accuracy, it is generally thought that HiFi reads will ultimately replace CLR for most human genome sequencing applications. However, the cost (TABLE 1) and computational resources required to generate HiFi data currently limit widespread adoption.

ONT long reads. ONT read lengths can surpass PacBio read lengths by at least an order of magnitude by generating continuous sequences hundreds to thousands of kilobases in length^{34–36}, although, in practice, such reads represent a small proportion of the total read length distribution. These enormous read lengths are facilitated by the unique pore chemistry essential to ONT sequencing,

a PacBio CLR and HiFi long reads



b ONT long and ultra-long reads



Polymerase reads

The sequence derived from one or more passes of the DNA polymerase around a SMRTbell template, including both adapters and inserts. Polymerase reads are trimmed to exclude any low-quality regions and are generated by Pacific Biosciences SMRT sequencing.

which allows molecules to translocate through the nanopore regardless of their length. Various studies have shown that the main factor limiting ONT read lengths is the extraction and preparation of high molecular weight DNA^{34–36}. These different methods of preparation underlie the two main types of ONT data: the standard long read (10–100 kb) read and the specialized ultra-long read (greater than 100 kb) (FIG. 3b).

The most common type of read generated via ONT sequencing is the standard ONT long read. Our meta-analysis indicates that these reads are typically 10–100 kb in length and 87–98% accurate, on average, although a

small portion can have an accuracy as low as 69% (FIG. 3c; Supplementary Fig. 1; Supplementary Note). About 91% of homopolymers at least five bases long are accurately called in raw ONT long reads, which is 3 percentage points higher than for PacBio CLR but approximately 8 percentage points lower than for PacBio HiFi reads (FIG. 3d; Supplementary Fig. 1; Supplementary Note). Our findings are consistent with previous reports^{34,36,56}. ONT raw read accuracy is highly dependent on the base-calling algorithm used^{38,57}, and recent improvements to these algorithms have increased raw read accuracy substantially in the past 5 years³⁸.

◀ **Fig. 3 | PacBio and ONT long-read data types.** **a** | The Pacific Biosciences (PacBio) platform can generate continuous long reads (CLRs) or high-fidelity (HiFi) reads. CLR data are generated by sequencing a SMRTbell template containing a DNA insert typically greater than 30 kb in length (yellow for forward strand, dark blue for reverse strand). Because of the large DNA insert size, the polymerase often completes only one or a few passes around the template. A base is incorrectly called in about 1 in every 10 bases, resulting in an error rate of 8–15% in the CLR. HiFi reads are generated by circular consensus sequencing (CCS) of a SMRTbell template containing a 10–30-kb DNA insert. The smaller insert size allows the polymerase to make several passes around the SMRTbell template. A consensus sequence is produced from the subreads, resulting in an error rate of 1% or less in the HiFi read. **b** | The Oxford Nanopore Technologies (ONT) platform can generate long or ultra-long reads. To generate long or ultra-long reads, high molecular weight (HMW) DNA is first extracted from cells or tissue. This extraction is commonly performed either with a commercially available DNA extraction kit, such as Qiagen's Puregene kit or Genomic-tip 500/G kit, or via traditional methods, such as a phenol–chloroform extraction followed by either an ethanol or 2-propanol precipitation. Kit-extracted DNA most often generates long reads (10–100 kb), whereas HMW DNA extracted by phenol–chloroform generates ultra-long reads (greater than 100 kb in length). **c** | Read length distributions and base accuracies of PacBio and ONT long-read data types differ. Shown are plots of the read length and accuracy distributions for PacBio HG002 CLR data generated with the Sequel II platform, PacBio CHM13 HiFi data generated with the Sequel II platform, ONT CHM13 long-read data generated with the PromethION and ONT ultra-long reads generated with the MinION and GridION. Read accuracy was estimated by aligning raw reads from each data type to the GRCh38 human reference genome and counting alignment differences as errors in the reads. Links to the publicly available datasets, a description of the methods used and the code required to reproduce the analysis are provided in Supplementary Note. A similar analysis was also performed in which raw reads were aligned to the Telomere-to-Telomere (T2T) consortium CHM13 assembly³⁴, and differences in alignment between the reads and the highly curated X chromosome were counted to estimate read accuracy. PacBio HiFi reads have a visibly higher read accuracy distribution when aligned to the T2T consortium CHM13 assembly than with GRCh38 because the high accuracy of the HiFi reads (greater than 99%) is sufficient to detect differences between the two genome assemblies, which are interpreted as base errors. The other long-read data types are not accurate enough to detect differences between the two genome assemblies. Consequently, the accuracy distribution for these other data types are similar (Supplementary Fig. 1a; Supplementary Note). **d** | Homopolymer accuracy differs between PacBio and ONT long-read data types. Shown is a plot of the homopolymer accuracy for the PacBio CLR, PacBio HiFi, ONT long-read and ONT ultra-long-read datasets used for part c. Homopolymer error was estimated by aligning raw reads from each data type to GRCh38 and comparing the observed homopolymer length in the reads with the homopolymer length. A similar analysis was performed where raw reads were aligned to the T2T consortium CHM13 assembly³⁴, and homopolymer error was estimated by comparison between the observed homopolymer length in the reads and the true homopolymer length in the highly curated X chromosome assembly. In both cases, homopolymers of at least five bases were assessed for accuracy (Supplementary Fig. 1b; Supplementary Note).

Read N50

The sequence length of the shortest read at 50% of the total sequencing dataset sorted by read length. In other words, half of the sequencing dataset is in reads larger than or equal to the read N50 size.

ONT long read

A read that is 10–100 kb in length and generated by Oxford Nanopore Technology (ONT) sequencing.

ONT ultra-long read

A read that is greater than 100 kb in length and generated by Oxford Nanopore Technology (ONT) sequencing.

Additionally, several methods have been developed to increase the consensus read accuracy of ONT long reads to ~97–98%, which is close to that of a PacBio HiFi read; these methods include INC-seq⁵⁸, HiFRE⁵⁹ and 1D2 sequencing⁶⁰.

Long-read data can be generated on any of the three standard ONT platforms: MinION, GridION, and PromethION. These three platforms differ in their flow cell capacity. The MinION, a pocket-sized device, can hold one flow cell, whereas the GridION can hold up to five flow cells, and the PromethION generates data from up to 48 flow cells at a time. Importantly, the MinION and the GridION use the same type of flow cell, with 2,048 individual nanopores split into 512 channels, whereas the PromethION uses a different type of flow cell with 12,000 nanopores split into 3,000 channels. Because each channel can perform sequencing with only one nanopore at a time, the MinION and GridION are

able to perform sequencing with 512 nanopores at a time per flow cell, while the PromethION is able to sequence ~5.9 times this amount (3,000 nanopores) at a time per flow cell. As a result, the PromethION provides nearly six times as much throughput per flow cell relative to the MinION or GridION, with 50–100 Gb of long-read data generated per PromethION flow cell³⁶ compared with 2–20 Gb generated per MinION or GridION flow cell^{34,35,56}. Because the PromethION can perform sequencing with up to 48 flow cells simultaneously, the PromethION throughput far exceeds that of the PacBio Sequel II and the Illumina NovaSeq (TABLE 1).

For low-throughput applications, ONT also offers the Flongle (or flow cell dongle), which is an adapter compatible with the MinION and GridION platforms. The Flongle uses a different type of flow cell that contains 126 nanopores in as many channels, allowing sequencing with all 126 nanopores at one time. A clear advantage of the Flongle is that it allows smaller, frequent and rapid tests to be performed at a fraction of the cost of MinION or GridION flow cells. Additionally, the portability of the Flongle and the MinION allow them to be transported in standard overhead lockers of aircraft and readily moved into the field without the need for complex and unwieldy instrumentation. The Flongle has been used in diverse clinical and field applications to detect influenza virus in clinical respiratory samples⁶¹ and diagnose lower respiratory tract infections⁶². Additionally, the MinION has been used to track small bacterial and viral genomes, such as those during the 2015 Ebola outbreak⁶³. Together, the portability and rapid sequencing speed of the Flongle and the MinION make them ideal for genomic sequencing applications in the field and the clinic.

ONT ultra-long reads. Another type of read that can be generated with ONT sequencing platforms is the ONT ultra-long read. These reads were first generated by Josh Quick³⁵ (see [Loman Labs](#)) and are typically greater than 100 kb in length^{34,35} but can be several megabases long³⁷. Our meta-analysis shows that read accuracy is similar for ONT ultra-long reads and ONT long reads: most reads average 87–98% accuracy, with a small fraction having a base accuracy as low as 68% (FIG. 3c; Supplementary Fig. 1; Supplementary Note), consistent with previously published reports^{34,35}. In addition, ultra-long reads have over 93% of homopolymers at least five bases long accurately called, similar to long reads (FIG. 3d; Supplementary Fig. 1; Supplementary Note). Although ultra-long reads shatter records with respect to read length, their throughput is much lower than that of standard long reads. Only 500 Mb to 2 Gb of ultra-long-read data are typically produced per flow cell with the MinION and the GridION, with a maximum throughput of 2.5 Gb (REFS^{34,35}). As a result, the generation of 20-fold ultra-long-read sequence data can take several weeks with a GridION platform when it is running at full capacity, which is substantially longer than the time it takes to generate standard ONT long-read data with the same device (TABLE 1). Attempts to generate ultra-long-read data on the PromethION have been met with limited success³⁶, which we speculate is because of

Table 2 | Statistics of human genome assemblies generated with various data types and assembly algorithms

Genome assembly	Data type (coverage, read N50 (kb))	Assembler	Size (Gb)	No. of contigs	Contig N50 (Mb)	Estimated cost (US\$)	Ref.
HGP (2001 draft)	Multitechnology ^a	GigAssembler, PHRAP	2.69	149,821	0.082	300,000,000	72
GRCh38 (hg38)	Multitechnology ^a	Multiple algorithms	3.01	998	57.88	Not determined	160
YH	Illumina (56x, <0.075)	SOAPdenovo	2.91	361,157	0.02	1,600 ^b	161
CHM13	PacBio CLR (77x, 17.5)	FALCON	2.88	1,916	29.30	2,700 ^c	30
		FALCON	3.00	2,116	31.92	4,100 ^c	52
	PacBio CLR (77x, 17.5) and ONT (50x, 70.4)	Canu	2.94	590	72.00	55,000 ^d	34
HG002	PacBio HiFi (28x, 13.5)	FALCON	2.91	2,541	28.95	2,700 ^c	53
		Canu	3.42	18,006	22.78		
	ONT (47x, 48.7)	Shasta	2.80	1,847	23.34	5,000 ^e	36
		Flye	2.82	1,627	31.25		
NA12878	Illumina (103x, 0.101)	ALLPATHS-LG	2.79	231,194	0.02	2,900 ^b	162
		Flye	2.82	782	18.18	4,000 ^e	76
		Canu	2.82	798	10.41		35
NA12878 (phased)	PacBio HiFi (30x, 10.0)	Peregrine	2.97 (H1)	9,334 (H1)	19.6 (H1)	4,100 ^c	22
			2.97 (H2)	9,127 (H2)	18.7 (H2)		
HG00733	ONT (73x, 29.6)	Shasta	2.78	2,150	24.43	6,000 ^d	36
		Flye	2.81	1,852	28.76		
		Canu	2.90	778	44.76		
HG00733 (phased)	PacBio HiFi (33x, 13.4) and Strand-seq (5x)	Peregrine	2.90 (H1)	2,618 (H1)	28.0 (H1)	9,000 ^f	91
			2.91 (H2)	2,557 (H2)	29.2 (H2)		

All cost estimates exclude the cost for labour, instrumentation, maintenance and computer resources. CLR, continuous long read; H1, first haplotype in the diploid genome assembly; H2, second haplotype in the diploid genome assembly; HGP, Human Genome Project; HiFi, high fidelity; ONT, Oxford Nanopore Technologies; PacBio, Pacific Biosystems. ^aClone-by-clone hierarchical sequencing with short and Sanger reads. ^bCurrent cost when generated with the Illumina NovaSeq 6000 using S4 flow cells and multiplexing. ^cCurrent cost when generated with the PacBio Sequel II. ^dCurrent cost when generated with the PacBio Sequel II and/or ONT GridION. ^eCurrent cost when generated with the ONT PromethION. ^fCurrent cost when generated with the PacBio Sequel II and Illumina HiSeq 2500.

the lack of compatible sequencing kits required to generate ultra-long reads. With improved kit compatibility, it is likely that ultra-long-read throughput will increase, improving ultra-long-read utility for whole-genome applications.

PacBio and ONT long-read and ultra-long-read sequencing data have begun to have a substantial impact on several areas of human genetics research, including genome assembly^{9,30,33–36,64}, variant discovery^{3,31,32,54}, disease association^{29,65–68} and human genetic diversity^{69–71}. New methods have evolved to apply the different long-read sequencing data types to each of these areas of research. In some cases, such as the complete assembly of human genomes, the different data types can be complementary.

Genome assembly with long reads

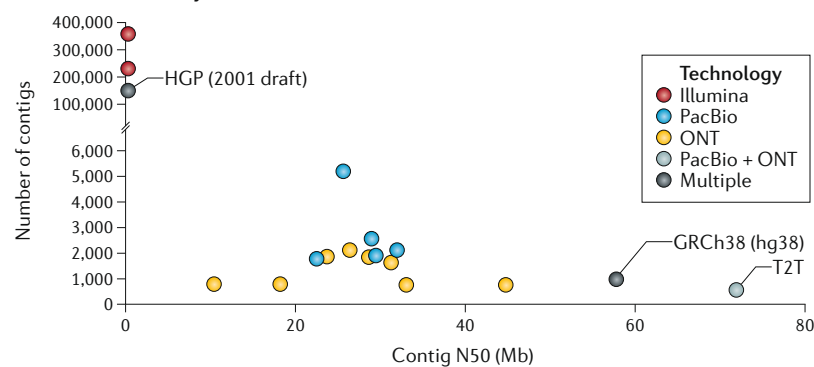
One of the first applications of long-read sequencing has been to improve the assembly of genomes, as read lengths are now sufficiently long to traverse most repeat structures of the genome. For diploid genomes, such as in humans, the challenge now is to achieve accurate haplotype resolution from telomere to telomere without guide from a reference.

De novo genome assembly. De novo genome assembly is the process by which randomly sampled sequence fragments are reconstructed to determine the order of every base in a genome⁷². Stitched-together sequence fragments are referred to as contigs, and in the ideal case, there is one contig per chromosome. Short-read technology has been problematic for the de novo assembly of mammalian genomes and has typically resulted in hundreds of thousands of gaps, owing to repetitive sequences that cannot be traversed by short reads. Numerous studies have shown that long-read genome assemblies are superior in their contiguity by orders of magnitude when compared with previous short-read and Sanger-based sequencing approaches^{30,32,33,35,70,71} (TABLE 2). For example, in early 2015, there were 99 mammalian genome assemblies in GenBank with an average contig N50 of only 41 kb, but none of them used long-read sequencing as the predominant data type²⁷. As of early 2020, there are more than 800 genome assemblies available through GenBank that used either PacBio or ONT data with contig N50 lengths greater than 5 Mb, including some of the first human genomes: NA12878 (REF.³⁵), CHM13 (REF.³²), HX1 (REF.⁷⁰) and AK1 (REF.⁷¹). This more than 100-fold increase in assembly

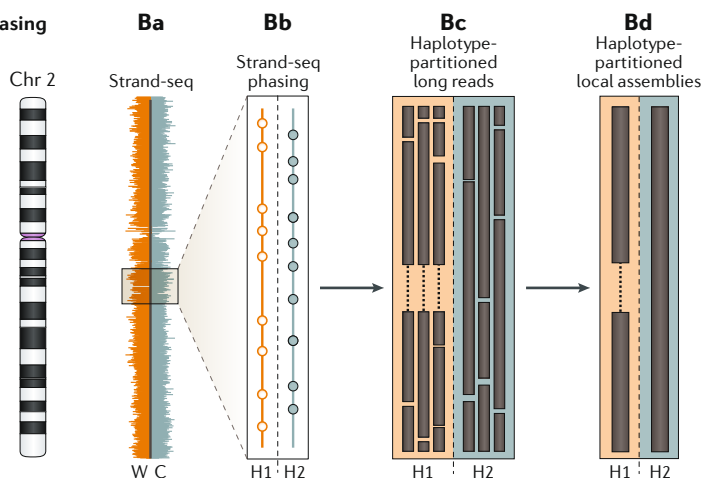
Contig N50

The sequence length of the shortest contig at 50% of the total genome length sorted by contig length. In other words, half of the genome sequence is contained in contigs larger than or equal to the contig N50 size.

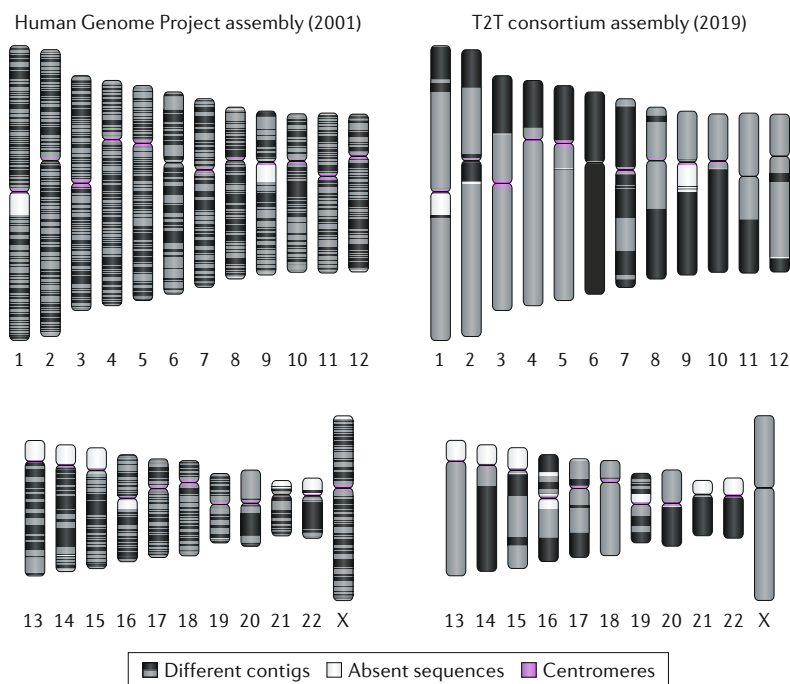
A Genome assembly



B Phasing



C Telomere-to-telomere chromosome assemblies



contiguity has been driven not only by longer reads but also by the development of genome assembly tools optimized for long-read data (such as Canu⁷³, HiCanu⁵⁵, Peregrine⁷⁴, FALCON⁷⁵, Flye⁷⁶, wtdbg2 (or RedBean)⁷⁷ and Shasta³⁶) and other tools that can increase assembly

Fig. 4 | Long-read data improve genome assembly.

A | The number of contigs and the contig N50 for 18 unphased human genome assemblies listed in TABLE 2. Genomes assembled from long-read data (PacBio Biosciences (PacBio) or Oxford Nanopore Technologies (ONT)) have fewer contigs and higher contig N50 values compared with those assembled from short-read data (Illumina). Combining long-read data types (PacBio and ONT) produces a genome assembly with even fewer contigs and a higher contig N50, surpassing that of the reference genome (GRCh38, hg38) in contiguity.

B | A genome assembly phasing approach known as Strand-seq¹⁶³. In this approach, the template strand (that is, the Watson (W, orange) or Crick (C, teal) strand) is sequenced via short-read sequencing to generate template-specific short reads. These reads are aligned to a genome assembly and binned in 200-kb genomic stretches (indicated by the orange and teal bars that align along the length of chromosome 2 (Chr 2); part **Ba**). Strand-seq reads may contain a single-nucleotide polymorphism that differentiates the homologue from its counterpart (part **Bb**), which can be used to partition long reads into either haplotype 1 (H1, empty circles) or haplotype 2 (H2, filled circles) (part **Bc**). Haplotype-partitioned long reads permit the detection of structural variation¹⁶⁴, such as the deletion in H1 (part **Bd**), and can be assembled into haplotigs that span the region, thereby generating phased genome assemblies^{88,165}.

C | Chromosome ideograms are shown that compare the 2001 Human Genome Project assembly⁷² and the 2019 Telomere-to-Telomere (T2T) consortium CHM13 assembly³⁴. The 2001 Human Genome Project assembly had more than 145,000 gaps and nearly 150,000 contigs, whereas the 2019 T2T consortium CHM13 assembly has fewer than 1,000 gaps and fewer than 1000 contigs (see TABLE 2 for additional statistics). Contigs are represented by alternating black and grey blocks, absent sequences are represented by white blocks and centromeres are represented by purple blocks. NCBI, National Center for Biotechnology Information.

contiguity and accuracy, such as optical mapping (for example, from Bionano Genomics)^{30,34,70,71,78} and electronic mapping (for example, from Nabsys)^{79,80}. Importantly, it is now becoming tractable for individual laboratories (as opposed to large consortia) to sequence and assemble human genomes in a few weeks at levels of contiguity approximate to or exceeding the level of the Human Genome Project^{31,36,81} (FIG. 4A). For example, Shafin et al. generated 11 highly contiguous (median NG50 of 18.5 Mb) human genome assemblies with long-read ONT data with only 3 PromethION flow cells and 6 hours of computer time on a 28-core machine with more than 1 TB of RAM per genome³⁶. Similarly, Chin and Khalak assembled human genomes in less than 100 minutes (30 CPU hours; not including the one-time computational cost of generating the PacBio HiFi reads) with a contig N50 greater than 20 Mb with only PacBio HiFi data⁷⁴. For comparison, an alignment of approximately 30-fold short-read Illumina data can take up to 100 CPU hours^{82,83}.

Polishing and phasing. Although speed is important, long-read genome assemblies have frequently been criticized for their reduced accuracy⁸³. However, with

Optical mapping

A technique commonly used to scaffold sequence contigs that involves constructing ordered genomic maps from single molecules of DNA with a fluorescent readout.

Electronic mapping

A technique commonly used to scaffold sequence contigs that involves constructing ordered genomic maps from single molecules of DNA with an electronic readout.

Phased de novo genome assembly

A genome assembly in which the maternal and paternal haplotypes are resolved.

Trio binning

A method in which short reads from two parental genomes are used to partition long reads from their offspring into haplotype-specific sets before the assembly of each haplotype.

Paralogous sequence variants

Single nucleotide differences between duplicated loci in the genome that are invariant in a population.

CHM13 human genome

A complete hydatidiform mole (CHM) genome that has lost the maternal genome and duplicated the paternal genome. This genome is currently the focus of the Telomere-to-Telomere (T2T) consortium's genome assembly efforts due to its essentially haploid nature and stable karyotype.

Whole-genome sequencing

Sequencing of the entire genome without using methods for sequencing selection.

proper correction and assessment, long-read assemblies can rival those generated by Illumina or Sanger sequencing⁸⁴. Unpolished assemblies typically suffer from many small indel errors, which complicate gene annotation⁵⁰. Most of these errors can be resolved with use of polishing tools (such as Racon⁴⁸, Nanopolish^{63,85,86}, MarginPolish³⁶, HELEN³⁶, Quiver⁴⁶, Arrow and Medaka) and error correction with short-read sequence data generated from the same individual⁴⁷. Recent developments in base-calling algorithms and the generation of highly accurate long-read sequence data types such as HiFi data are eliminating dependencies on short-read data polishing^{52,53,84}. A major focus moving forward is the generation of high-quality, fully phased diploid genomes where both haplotypes are represented⁸⁴. This procedure essentially converts a 3-Gb collapsed human genome into a 6-Gb genome that represents both maternal and paternal complements, which has the advantage of increasing overall sensitivity for variant discovery⁹. Fortunately, phased de novo genome assembly is now becoming feasible with new strategies that take advantage of parental information to phase long reads (such as trio binning)⁸⁷, computational methods that take advantage of the inherent phasing present in long-read data (such as FALCON-Unzip)⁷⁵ and methods that apply orthogonal technologies to phase single-nucleotide polymorphisms in long-read data (such as Strand-seq^{9,88,89}, Hi-C⁹⁰ and, in the past, 10x Genomics⁹) (FIG. 4B). The fundamental concept here is straightforward: by physically or genetically phasing an individual genome, the long-read data can be partitioned into two parental genome datasets that can be independently assembled. Such a procedure is particularly valuable for resolving structural variation and its haplotype architecture⁹¹ because structural differences between haplotypes have often led to hybrid representations or collapses in the assembly that do not reflect the true sequence and are, therefore, biologically meaningless⁹².

Telomere-to-telomere chromosome assemblies. The ultimate genome assembly is a single contig per chromosome, where the order and orientation of the complete chromosome sequence are resolved from telomere to telomere. More than half of the remaining gaps in long-read genome assemblies correspond to regions of segmental duplications^{27,52,54,91} and can be readily identified by increased read depth. These collapses result from a failure to resolve highly identical sequences. However, these regions can be assembled with greater than 99.9% accuracy with use of approaches that partition the underlying long reads using a graph of paralogous sequence variants⁹³, such as use of Segmental Duplication Assembler⁵⁴. The human reference genome has been the gold standard for mammalian genomes since its first publication in 2001, and there has been considerable investment over the past two decades to increase its accuracy and contiguity. Notwithstanding, even in its current iteration (GRCh38, or hg38), the number of contigs greatly exceeds the number of chromosomes (998 contigs versus 24 chromosomes), with most of the major gaps corresponding to large repetitive sequences present in centromeres, acrocentric DNA

and segmental duplications (TABLE 2). Application of ONT and PacBio technologies to the essentially haploid CHM13 human genome has shown that we are on the cusp of generating telomere-to-telomere genome assemblies. By combining both of these sequencing data types with improved assembly algorithms, Miga and colleagues showed that it is possible to represent the CHM13 human genome as 590 contigs, including a complete telomere-to-telomere assembly of the X chromosome³⁴ (FIG. 4C; TABLE 2). Key to this advance was the generation of high-coverage ultra-long ONT data, which allowed greater contiguity than GRCh38 (81.3 Mb versus 57.9 Mb) and, for the first time, a reconstruction of the highly repetitive centromeric α -satellite array on the X chromosome. However, the telomere-to-telomere assembly process is far from automated, requiring considerable manual curation, and hundreds of collapsed repeats still remain to be resolved genome-wide. Nevertheless, efforts to automate centromere assembly (such as with CentroFlye⁹⁴ and HiCanu⁵⁵) are under way. Further developments, such as improved assembly tools that optimize the processing and assembly of PacBio HiFi sequence data or that couple them to ONT ultra-long-read data, will be required before telomere-to-telomere chromosome assemblies can be routinely generated for diploid genomes. Routine and accurate telomere-to-telomere assembly of human chromosomes from diploid genomes will likely take years, not just because specialized data types (that is, ultra-long-read sequence reads) are more expensive and take longer to generate, but also because it will involve uncharted territories of the human genome. For many regions, including centromeric, acrocentric and large regions of segmental duplication, the sequence has not been correctly assembled even once, so any computational assembly algorithm geared to such regions^{54,94} will require painstaking validation and assessment.

Understanding variation with long reads

Increased accuracy and contiguity of genome assemblies necessarily enhances our understanding of more complex forms of genetic variation, and this, in turn, improves our understanding of mutation and evolutionary processes.

Large-scale structural variant detection and disease.

Long-read genome sequencing has substantially enhanced our understanding of the full spectrum of human genetic variation^{32,33,64}. A comparison of the same individuals sequenced with the Illumina short-read and PacBio long-read platforms, for example, showed that 47% of the deletions and nearly 78% of insertions were missed by Illumina whole-genome sequencing even after application of 11 different variant callers designed to detect insertions, deletions, inversions and duplications in genomes⁹. Most of the gains in sensitivity involve intermediate-size variants ranging from 50 bp to 2 kb in length. Additionally, an analysis of difficult-to-assay sequences from 748 human genes, for which mapping quality is low for some individual protein-coding exons with Illumina-based exome sequencing, reported remarkable increases in sensitivity with long-read

sequencing, including the discovery of potentially pathogenic variants associated with Alzheimer disease⁹⁵. Similarly, there is evidence of increased sensitivity for the detection of indels of less than 50 bp in length^{30,96}, although this effect has been more difficult to quantify due to the predominant error types in long-read data. Accompanying this increase in sensitivity has been a spate of new structural variant callers (SMRT-SV³³, MsPAC⁹³, Phased-SV⁹, Sniffles⁹⁷ and PBSV⁵³) designed to discover, sequence and, in some cases, phase structural variants on the basis of specific long-read sequence signatures and local assembly. These callers rely on the alignment of long-read data to a reference genome via specialized algorithms (such as BLASR⁹⁸, NGMLR⁹⁷, minimap2 (REF.⁹⁹) and MHAP¹⁰⁰); however, as the speed and accuracy of generating fully phased and assembled human genomes increase, it is likely that many of these discovery tools will be supplanted by direct comparisons of assembled genomes for variant discovery³⁰. Although there have been substantial gains in variant discovery, particular classes, including large copy number variants and inversions mapping within or near large segmental duplications, are still difficult to resolve solely with existing long-read technology⁹.

An immediate application of this increased sensitivity has been the discovery and sequencing of more complex forms of disease-causing variation^{56,101–108}, including novel GGC repeat expansions associated with neuronal intranuclear inclusion disease and adults with leukoencephalopathy^{65,66,109}, founder SVA retrotransposon insertions responsible for X-linked dystonia–parkinsonism in the Philippines¹¹⁰, novel candidate mutations associated with schizophrenia and bipolar disorder¹¹¹, pentanucleotide repeat expansions linked to familial and sporadic cases of benign adult myoclonic epilepsy in Japan and China^{103,109} and the discovery of large complex triplications and regions of segmental uniparental disomy associated with Temple syndrome¹¹². Here too, specialized algorithms have been developed to detect and accurately predict short tandem repeat expansions as well as predict methylation status of the flanking regions from underlying long-read sequence data (for example, STRique)¹¹³. Expanding catalogues of sequence-resolved structural variation are identifying new lead variants associated with both expression quantitative trait loci and genome-wide association studies³¹ and suggesting candidate loci for repeat-associated instability diseases¹¹⁴. Importantly, these discoveries are leading to new insights regarding disease mechanisms, such as the reported finding that TTTCA repeat expansions within introns are associated with myoclonic epilepsy irrespective of the protein-coding gene in which they are found, potentially because of RNA-mediated toxicity linked to their transcription¹¹⁵. It is worth noting that the layers of genomic complexity and structural variation revealed only through high-quality sequencing often yield insights into multiple diverse diseases. For example, the GGC repeat expansion associated with *NOTCH2NLC* and neuronal intranuclear inclusion disease maps to human-specific segmental duplications on chromosome band 1q21 that have recently been implicated in cortical neurogenesis and expansion of the frontal cortex

during human evolution^{116,117}. The presence of these duplications was used to predict and discover recurrent rearrangements associated with developmental delay, microcephaly and macrocephaly^{68,118,119} and later schizophrenia⁶⁷ (FIG. 5a). Mapping-based approaches, rather than whole-genome assembly, were used in these studies to discover and resolve the structure of the variants in question^{65,101}. Yet, these discoveries were often preceded by high-quality assembly of the gene model or the locus of interest, which were missing from the original human genome but now can be assembled with use of whole-genome assembly methods⁵⁴. Mapping-based approaches are largely ineffective without high-quality references for comparison.

Human genetic diversity and evolution. Implicit in the sequencing and assembly of new human genomes and in increased structural variation discovery is an improved understanding of human genetic diversity and the mutational processes that have shaped our genomes^{31–36,53,64,70,71,78,81,90} (FIG. 5b). For example, long-read sequencing of a modest diversity panel of 15 human genomes identified almost 100,000 structural variants — most of which were previously unknown³¹. Among these, variable number tandem repeats were shown to be the most non-randomly distributed, with almost half mapping to the last 5 Mb of subtelomeric regions, possibly owing to increased rates of double-strand breaks in these regions³¹. Comparison of human and non-human primate genomes sequenced with PacBio technology have doubled the number of structural variants associated with brain expression differences specific to the human lineage³⁰ and identified large-scale changes potentially important in the evolution of ape lineages¹²⁰. Recent sequencing and assembly of large copy number polymorphisms have identified structural variants associated with both positive selection and introgression that are largely specific to certain human populations⁶⁹. For example, a 386-kb duplication polymorphism was fully sequenced and assembled that is effectively specific to individuals of Melanesian descent. Remarkably, the duplication, as well as the duplicated genes within, arose in the archaic Denisovan lineage and was subsequently introgressed back into the human ancestor through interbreeding. The duplication shows multiple signatures of positive selection and is now present in 79% of Melanesians but is virtually absent in other populations. The discovery and sequencing of such complex structural variants further improves genotyping even among short-read datasets, making it feasible to enhance association studies^{31,32}. For this reason, the US National Institutes of Health (NIH) recently launched an initiative, the Human Pangenome Reference Sequence Project, to sequence and assemble more than 350 diverse human genomes using long-read sequencing platforms¹²¹.

Beyond DNA sequencing

In addition to genome assembly and variant discovery, long-read sequencing has been applied to molecules other than DNA, making possible the detection, for example, of full-length RNA isoforms^{122–124} as well as modifications of native RNA and DNA^{96,125–127}.

SVA

A type of retrotransposon insertion composed of a (CCCTCT)_n hexamer simple repeat region at the 5' end, an *Alu*-like region, a variable number of tandem repeat (VNTR) region, a short interspersed element of retroviral origin (SINE-R) region, and a poly(A) tail after the putative polyadenylation signal.

Uniparental disomy

Inheritance of two copies of a chromosome or segments of a chromosome from one parent, instead of one copy from each parent.

Expression quantitative trait loci

Loci that explain a fraction of the genetic variant of a gene expression phenotype.

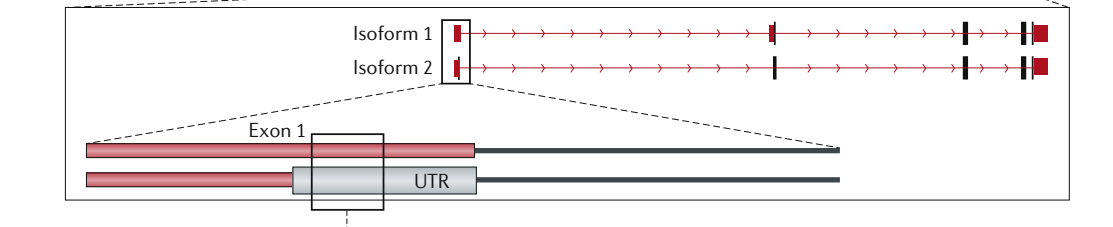
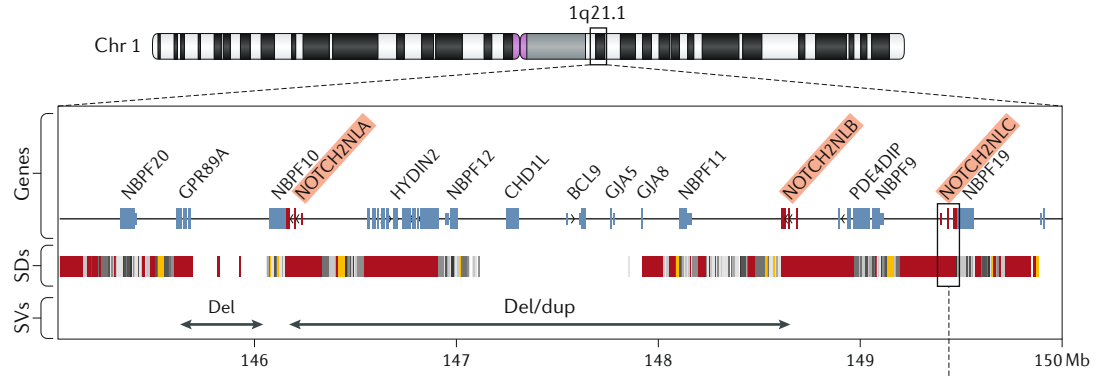
Genome-wide association studies

An approach used in genetics research to associate specific genetic variations with particular traits.

Introgression

The transfer of genetic information from one species to another as a result of hybridization between them and repeat backcrossing.

a Structural variation



GGC repeat expansion

Normal: 1 25 45
 Expansion: 1 25 50 75 76 100 125 150 151 175 200 225 226 250 275 300 301 325 350 375 376 400 425 430

Diseases associated with the GGC repeat expansion: neuronal intranuclear inclusion disease and leukoencephalopathy

b Human evolution and diversity

Macaque, brain tissue Chimpanzee, cerebral organoid Human, cerebral organoid Human, brain tissue

Genes near structural variants

Derived expression differences

Chimpanzee: High gene expression (Enhancer region, Exon 1, Exon 2, Exon 3)

Human: Low gene expression (Human-specific deletion, Exon 1, Exon 2, Exon 3)

◀ **Fig. 5 | Long-read data provide insights into the biological relevance of structural variation and human evolution and diversity.** **a** | The *NOTCH2NLA*, *NOTCH2NLB*, and *NOTCH2NLC* genes are located within chromosome band 1q21.1, a segmental duplication (SD)-rich region of the genome partially assembled by Pacific Biosciences (PacBio) continuous long read (CLR) sequencing of bacterial artificial chromosome clones¹¹⁶. The region was originally incorrectly assembled in the human reference genome¹¹⁶. Deletions (del) and duplications (dup) mediated by the SD-rich region can cause thrombocytopenia-absent radius syndrome¹⁶⁶ as well as distal 1q21.1 deletion/duplication syndrome^{119,167}. High-quality sequencing of the region allowed the breakpoints of these disease-causing rearrangements to be better defined and improved the annotation of human-specific *NOTCH2NL* duplicate genes¹¹⁶. Subsequent sequencing of this region in patients with neuronal intranuclear inclusion disease and leukoencephalopathy by PacBio and Oxford Nanopore Technologies long-read sequencing recently identified a GGC repeat expansion in exon 1 of *NOTCH2NLC* in affected patients⁶⁶ (exons are in red, untranslated regions (UTRs) are in grey). Expansion of the repeat is associated with the production of antisense transcripts whose role is uncertain but may interfere with the expression and regulation of the gene family. **b** | The panel on the left shows a heatmap of differentially expressed genes located near structural variants (SVs) in chimpanzees and humans. Differences in macaque, chimpanzee and human brains for genes that have a human-specific SV within 50 kb of the transcription start or stop site. Structural changes, such as a deletion of an enhancer region as shown on the right, can cause changes in gene expression fundamental to brain development³⁰. Part **a** is adapted from REF.⁶⁶, Springer Nature Limited.

Full-length RNA sequencing. A major strength of long-read sequencing technology is the ability to determine the sequence of full-length RNA transcripts arising from genes. PacBio sequencing technology and ONT sequencing technology are both able to resolve the sequence of full-length RNA molecules, either via cDNA sequencing (PacBio and ONT)^{128–131} or via native RNA sequencing (ONT)^{122–124}. Such sequence data improves gene annotation and simplifies downstream analysis by eliminating the need to reconstruct isoforms based on the error-prone assembly of short RNA-sequencing reads. The primary method used by PacBio to identify full-length RNA molecules is Iso-Seq¹²⁹, which involves cDNA synthesis, PCR amplification and SMRTbell ligation followed by CCS. The Iso-Seq method has been successfully used to capture novel isoforms^{54,70,71,129,132} and validate new gene models⁵⁴ in diverse genomes⁶⁹ (FIG. 6a). Similar to the CCS mode of PacBio, ONT has developed rolling circular amplification of concatemeric sequences (known as R2C2) as a means to increase the accuracy of cDNA sequence¹³³. In contrast to PacBio sequencing technology, which depends on cDNA synthesis, ONT sequencing technology can be applied to native RNA molecules to capture the full-length isoforms¹²². Native RNA sequencing has the advantage that it ensures all RNA molecules are captured, including long transcripts often missed during cDNA synthesis owing to their length or complexity¹³⁰. Furthermore, it avoids sequence biases frequently introduced during PCR amplification of cDNA¹³⁴. Full-length poly(A) transcriptomes have been readily obtained by ONT native RNA sequencing^{123,124}. Additionally, native RNA sequencing has revealed novel isoforms arising from disease-risk genes associated with psychiatric disorders¹³⁵ and chronic lymphoid leukaemia¹³⁶, which may provide new targets for early disease detection in clinical settings and for pharmaceutical treatments.

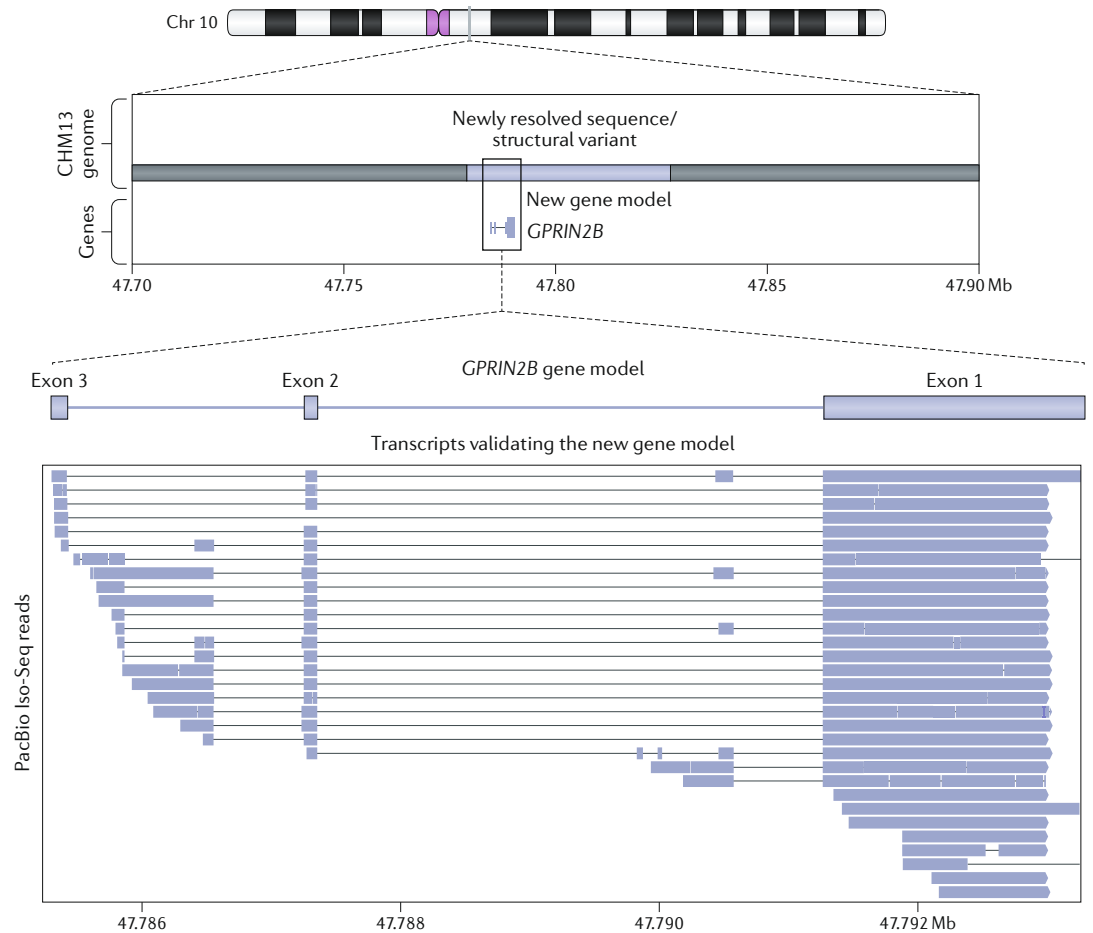
DNA and RNA methylation detection. Because PacBio sequencing technology and ONT sequencing technology both target native unamplified templates for sequencing,

the DNA and RNA molecules retain base modifications, allowing epigenomic changes to be detected through polymerase kinetics^{96,125,126,137} or current changes, respectively^{86,126,127}. Before the development of these technologies, the most common base modification that could be detected was methylated cytosine, with use of an indirect approach known as bisulfite sequencing. With bisulfite sequencing, DNA is treated with bisulfite, which converts cytosine to uracil but leaves modified cytosines unaffected. Short-read sequencing of the resulting DNA along with an untreated control allows the identification of modified cytosines. However, it does not discriminate between different types of cytosine modifications¹³⁸ nor does it allow the detection of other modified bases. Native DNA and RNA sequencing via PacBio and/or ONT technology presents substantial advantages over standard bisulfite-based sequencing methods because it allows a more diverse array of modifications to be identified, including 4-methylcytosine, 5-methylcytosine, 5-hydroxymethylcytosine, *N*⁶-methyladenine and 8-oxoguanine^{127,139–144}. Additionally, direct sequencing of native molecules simplifies the process by eliminating the need to prepare bisulfite-treated samples that are sequenced separately from the untreated samples¹⁴⁵. Similarly, long-read sequencing technologies greatly facilitate the detection of modified RNA bases by eliminating the use of highly specialized protocols to detect diverse types of modifications^{146–149}. Thus, direct sequencing of native DNA and RNA molecules is expanding the fields of epigenomics and epitranscriptomics by allowing the detection of previously unrecognized modifications on DNA and RNA concurrent with sequencing.

To detect modifications on DNA, PacBio technology depends on detecting changes in polymerase kinetics during SMRT sequencing^{96,125,126,137}. Kinetic characteristics, such as the arrival time and duration between two successive base incorporations, yield information about polymerase or reverse transcriptase kinetics that facilitate base modification detection. Because various modifications affect polymerase kinetics differently, SMRT sequencing can identify these kinetic signatures at base pair resolution but typically requires high sequence coverage (25-fold to 250-fold) to do so¹³⁹. Targeted enrichment of select DNA loci via CRISPR–Cas9 (REFS^{150,151}) has shown promise for achieving the higher sequence coverage needed for accurate base modification detection. PacBio SMRT sequencing has led to the discovery of methylation profile differences in diseased and healthy individuals¹⁰⁹ and has been used to identify novel hypermethylated regions in the genome¹⁵². For example, Ishiura and colleagues found that novel CGG repeat expansions associated with neural intranuclear inclusion disease were hypermethylated when compared with their unexpanded counterparts¹⁰⁹. Additionally, Suzuki and colleagues uncovered novel long interspersed nuclear elements that were methylated in the human genome, which were previously missed with bisulfite sequencing¹⁵².

ONT sequencing is also able to detect modifications on native DNA and RNA molecules with high accuracy owing to the characteristic current disruption caused by

a Transcriptome sequencing



b Methylation detection

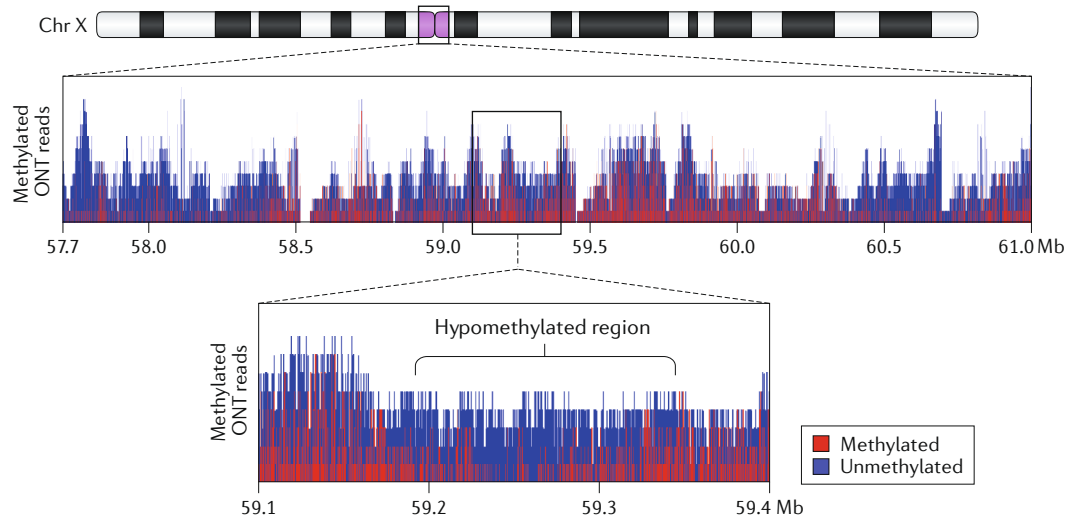


Fig. 6 | Long-read platforms can be used to sequence RNA and detect nucleic acid modifications. a | Long-read RNA sequencing can be used for full-length isoform discovery. A newly resolved sequence in chromosome 10 (Chr 10) of the CHM13 genome revealed a previously undiscovered gene, *GPRIN2B*. With use of Pacific Biosciences (PacBio) Iso-Seq method, full-length transcripts were identified that completely span *GPRIN2B*, validating the new gene model⁵⁴. **b** | The assembly of the entire X chromosome (Chr X) centromere revealed that the majority of the α -satellite repeat region is heavily methylated, except for an ~93-kb hypomethylated region³⁴. This finding was discovered via Oxford Nanopore Technologies (ONT) long-read sequencing of native DNA molecules and subsequent analysis with the methylation detection tool Nanopolish⁸⁶. Part **a** is adapted from REF.⁵⁴, Springer Nature Limited.

the modified base as it translocates through the nanopore^{86,126,127,142}. Several computational tools have been developed to detect DNA and RNA modifications on the basis of these characteristic disruptions: Nanopolish^{85,86}, signalAlign¹²⁷, DeepSignal¹⁵³, mCaller¹⁵⁴, DeepMod¹⁵⁵ and Tombo¹⁵⁶. These tools have been used to uncover methylation states in previously inaccessible regions of the genome and transcriptome, such as the X chromosome centromere³⁴ (FIG. 6b), as well as genes implicated in cancer¹⁵⁷, leading to new biological insights. In particular, the finding that the human X chromosome centromere is methylated across the entire DXZ2 α -satellite repeat array except for an ~93-kb pocket of hypomethylation suggests differences in epigenetic regulation in these repeat-dense regions³⁴. Additionally, the discovery that structural variants are differentially methylated in cancer cells is providing insight into the complex epigenetic characteristics of structurally variant regions implicated in cancer¹⁵⁷. As more and more phased human genome assemblies become available, it may become possible to determine the methylation status of each allele, which could lead to important discoveries that lie at the root of allelic epigenetic variation.

Conclusions and future perspectives

Sequencing technology is the ‘microscope’ by which geneticists study genetic variation, and it is clear that long-read technologies have provided us with a new ‘lens and objective’ for understanding DNA and RNA variation, structure and organization. Although the two predominant long-read technologies are competitive, some of the best results have been obtained when the sequencing platforms are used to complement one another. For example, the first telomere-to-telomere assembly of the human X chromosome leveraged both the accuracy of deep PacBio CLR data and ONT ultra-long-read data to traverse centromeric regions. ONT sequencing generates the longest contiguous sequence reads and is the most portable, whereas PacBio sequencing produces some of the most accurate long-read data and is beginning to rival next-generation sequencing. Both technologies use

native DNA as opposed to amplified products as templates for sequencing and thus provide access to more uniform and biologically meaningful data. Continued reductions in cost, increases in accuracy and increases in throughput will make these technologies more commonplace in the laboratory, field and clinic. With the ability to now sequence, assemble and phase human genomes at levels of contiguity exceeding that of the Human Genome Project for a few thousand dollars, the field of human genetics has forever changed. We are now embarking on an era where all genetic variation in an individual will be completely discovered in the next few years. Hundreds and ultimately thousands of new human reference genomes will be produced. In addition, light sampling (~10-fold to 15-fold sequence coverage) of thousands of individuals (such as in a project in Iceland¹⁵⁸ and the NIH-funded *All of Us* project in the USA) provides an alternative strategy for improved variant discovery from a population perspective¹⁵⁸. These advances will dramatically improve our understanding of human heritability, population diversity and mutational processes and the genetic basis of disease. Notably, adoption of long-read technology will also change how we discover and catalogue human variation. Variation will be discovered not by simply aligning reads to a single reference genome and inferring genetic differences but rather by sequencing and assembling complete haplotypes for which complex genetic variation is fully sequence resolved. The next steps will likely involve the development of graph-based reference genomes using new standards, such as Variant Graph Toolkit¹⁵⁹. Functional data will be superimposed on these complete genomes, including epigenetic and transcriptomic differences that occur ultimately at the cellular and developmental level.

The wealth of additional information afforded by single-molecule, long-read sequencing compared with short-read sequencing promises a more comprehensive understanding of genetic, epigenetic and transcriptomic variation and its relationship to human phenotype.

Published online 5 June 2020

- van Dijk, E. L., Jaszczyszyn, Y., Naquin, D. & Thermes, C. The third revolution in sequencing technology. *Trends Genet.* **34**, 666–681 (2018).
- Shendure, J. et al. DNA sequencing at 40: past, present and future. *Nature* **550**, 345–353 (2017).
- Sudmant, P. H. et al. An integrated map of structural variation in 2,504 human genomes. *Nature* **526**, 75–81 (2015).
- Sudmant, P. H. et al. Global diversity, population stratification, and selection of human copy-number variation. *Science* **349**, aab3761 (2015).
- Ng, S. B. et al. Exome sequencing identifies MLL2 mutations as a cause of Kabuki syndrome. *Nat. Genet.* **42**, 790–793 (2010).
- Kircher, M. et al. A general framework for estimating the relative pathogenicity of human genetic variants. *Nat. Genet.* **46**, 310–315 (2014).
- Simonson, T. S. et al. Genetic evidence for high-altitude adaptation in Tibet. *Science* **329**, 72–75 (2010).
- Sudmant, P. H. et al. Diversity of human copy number variation and multicopy genes. *Science* **330**, 641–646 (2010).
- Chaisson, M. J. P. et al. Multi-platform discovery of haplotype-resolved structural variation in human genomes. *Nat. Commun.* **10**, 1784 (2019). **This study compares multiple sequence and mapping technologies for the genomes of three parent-child trios and quantifies the amount of missing genetic variation. A method, Phased-SV, is developed that partitions long-read data on the basis of phased single-nucleotide polymorphisms, which resolves the sequence of both structural haplotypes.**
- 1000 Genomes Project Consortium. et al. A global reference for human genetic variation. *Nature* **526**, 68–74 (2015).
- Bailey, J. A., Yavor, A. M., Massa, H. F., Trask, B. J. & Eichler, E. E. Segmental duplications: organization and impact within the current human genome project assembly. *Genome Res.* **11**, 1005–1017 (2001).
- Hodgkinson, A., Chen, Y. & Eyre-Walker, A. The large-scale distribution of somatic mutations in cancer genomes. *Hum. Mutat.* **33**, 136–143 (2012).
- Hills, M., Jeyapalan, J. N., Foxon, J. L. & Royle, N. J. Mutation mechanisms that underlie turnover of a human telomere-adjacent segmental duplication containing an unstable minisatellite. *Genomics* **89**, 480–489 (2007).
- Hastings, P. J., Lupski, J. R., Rosenberg, S. M. & Ira, C. Mechanisms of change in gene copy number. *Nat. Rev. Genet.* **10**, 551–564 (2009).
- Zheng, G. X. Y. et al. Haplotyping germline and cancer genomes with high-throughput linked-read sequencing. *Nat. Biotechnol.* **34**, 303–311 (2016).
- Zhang, F. et al. Haplotype phasing of whole human genomes using bead-based barcode partitioning in a single tube. *Nat. Biotechnol.* **35**, 852–857 (2017).
- Wang, O. et al. Efficient and unique cobarcode of second-generation sequencing reads from long DNA molecules enabling cost-effective and accurate sequencing, haplotyping, and de novo assembly. *Genome Res.* **29**, 798–808 (2019).
- Li, R. et al. Illumina synthetic long read sequencing allows recovery of missing sequences even in the “finished” *C. elegans* genome. *Sci. Rep.* **5**, 10814 (2015).
- Peters, B. A. et al. Accurate whole-genome sequencing and haplotyping from 10 to 20 human cells. *Nature* **487**, 190–195 (2012).
- Lieberman-Aiden, E. et al. Comprehensive mapping of long-range interactions reveals folding principles of the human genome. *Science* **326**, 289–293 (2009).
- Ghurye, J. et al. Integrating Hi-C links with assembly graphs for chromosome-scale assembly. *PLoS Comput. Biol.* **15**, e1007273 (2019).
- Garg, S. et al. Efficient chromosome-scale haplotype-resolved assembly of human genomes. Preprint at *bioRxiv* <https://doi.org/10.1101/810341> (2019).
- Harewood, L. et al. Hi-C as a tool for precise detection and characterisation of chromosomal rearrangements and copy number variation in human tumours. *Genome Biol.* **18**, 125 (2017).

24. Chu, J., Mohamadi, H., Warren, R. L., Yang, C. & Birol, I. Innovations and challenges in detecting long read overlaps: an evaluation of the state-of-the-art. *Bioinformatics* **33**, 1261–1270 (2017).
25. Jung, H., Winefield, C., Bombarely, A., Prentis, P. & Waterhouse, P. Tools and strategies for long-read sequencing and de novo assembly of plant genomes. *Trends Plant Sci.* **24**, 700–724 (2019).
26. Sedlazeck, F. J., Lee, H., Darby, C. A. & Schatz, M. C. Piercing the dark matter: bioinformatics of long-range sequencing and mapping. *Nat. Rev. Genet.* **19**, 329–346 (2018).
27. Chaisson, M. J. P., Wilson, R. K. & Eichler, E. E. Genetic variation and the *de novo* assembly of human genomes. *Nat. Rev. Genet.* **16**, 627–640 (2015).
28. Pollard, M. O., Gurdasani, D., Mentzer, A. J., Porter, T. & Sandhu, M. S. Long reads: their purpose and place. *Hum. Mol. Genet.* **27**, R234–R241 (2018).
29. Mantere, T., Kersten, S. & Hoischen, A. Long-read sequencing emerging in medical genetics. *Front. Genet.* **10**, 426 (2019).
30. Kronenberg, Z. N. et al. High-resolution comparative analysis of great ape genomes. *Science* **360**, eaar6343 (2018).
31. Audano, P. A. et al. Characterizing the major structural variant alleles of the human genome. *Cell* **176**, 663–675.e19 (2019).
This article provides a large catalogue of sequence-resolved structural variants based on long-read sequence analysis of a diverse panel of 15 genomes and identifies instances where the human reference has a minor allele for a structural variant. It also develops a machine learning-based approach for genotyping sequence-resolved structural variants in Illumina whole-genome shotgun sequence data, which led to the discovery of expression quantitative trait loci and new lead variants for genome-wide association studies.
32. Huddleston, J. et al. Discovery and genotyping of structural variation from long-read haploid genome sequence data. *Genome Res.* **27**, 677–685 (2017).
33. Chaisson, M. J. P. et al. Resolving the complexity of the human genome using single-molecule sequencing. *Nature* **517**, 608–611 (2015).
This article describes one of the first methods for sequencing and assembling structural variation from long-read sequence data. It shows that most of these variants are novel, and thus a large amount of human genetic variation is missed with short-read sequencing approaches.
34. Miga, K. H. et al. Telomere-to-telomere assembly of a complete human X chromosome. Preprint at *bioRxiv* <https://doi.org/10.1101/735928> (2019).
This landmark study shows that PacBio and ONT long reads are able to generate a *de novo* genome assembly superior in contiguity to all other genome assemblies (including hg38). Importantly, it reveals the first telomere-to-telomere sequence assembly of a human chromosome and shows that it is possible to resolve megabase-sized arrays of near-identical tandem repeats (that is, the centromere) with long and ultra-long reads.
35. Jain, M. et al. Nanopore sequencing and assembly of a human genome with ultra-long reads. *Nat. Biotechnol.* **36**, 338–345 (2018).
This article demonstrates that ONT ultra-long reads can be used for *de novo* human genome assembly. Additionally, this assembly resolved both haplotypes of the human major histocompatibility locus for the first time.
36. Shafin, K. et al. Nanopore sequencing and the Shasta toolkit enable efficient *de novo* assembly of eleven human genomes. *Nat. Biotechnol.* <https://doi.org/10.1038/s41587-020-0503-6> (2020).
This study describes the rapid assembly of 11 human genomes using ONT long reads, and it debuts a new assembler (Shasta) and polisher (HELEN). This article provides the methodological basis for scalability in human genome assembly using long reads.
37. Payne, A., Holmes, N., Rakyau, V. & Loose, M. BulkVis: a graphical viewer for Oxford Nanopore bulk FAST5 files. *Bioinformatics* **35**, 2193–2198 (2019).
38. Rang, F. J., Kloosterman, W. P. & de Ridder, J. From squiggle to basepair: computational approaches for improving nanopore sequencing read accuracy. *Genome Biol.* **19**, 90 (2018).
39. Ardui, S., Ameer, A., Vermeesch, J. R. & Hestand, M. S. Single molecule real-time (SMRT) sequencing comes of age: applications and utilities for medical diagnostics. *Nucleic Acids Res.* **46**, 2159–2168 (2018).
40. Carneiro, M. O. et al. Pacific Biosciences sequencing technology for genotyping and variation discovery in human data. *BMC Genomics* **13**, 375 (2012).
41. Eid, J. et al. Real-time DNA sequencing from single polymerase molecules. *Science* **323**, 133–138 (2009).
42. Korfach, J. Understanding accuracy in SMRT® sequencing. *PacBio* https://www.pacb.com/wp-content/uploads/2015/09/Perspective_UnderstandingAccuracySMRTSequencing.pdf (2015).
43. Rhoads, A. & Au, K. F. PacBio sequencing and its applications. *Genomics Proteomics Bioinformatics* **13**, 278–289 (2015).
44. Weirather, J. L. et al. Comprehensive comparison of Pacific Biosciences and Oxford Nanopore Technologies and their applications to transcriptome analysis. *F1000Res* **6**, 100 (2017).
45. Fox, E. J., Reid-Bayliss, K. S., Emond, M. J. & Loeb, L. A. Accuracy of next generation sequencing platforms. *Next Gener. Seq. Appl.* **1**, 1000106 (2014).
46. Chin, C.-S. et al. Nonhybrid, finished microbial genome assemblies from long-read SMRT sequencing data. *Nat. Methods* **10**, 563–569 (2013).
47. Walker, B. J. et al. Pilon: an integrated tool for comprehensive microbial variant detection and genome assembly improvement. *PLoS One* **9**, e112963 (2014).
48. Vaser, R., Sović, I., Nagarajan, N. & Šikić, M. Fast and accurate *de novo* genome assembly from long uncorrected reads. *Genome Res.* **27**, 737–746 (2017).
49. Garrison, E. & Marth, G. Haplotype-based variant detection from short-read sequencing. Preprint at *arXiv* <https://arxiv.org/abs/1207.3907> (2012).
50. Gordon, D. et al. Long-read sequence assembly of the gorilla genome. *Science* **352**, aae0344 (2016).
51. Hu, J., Fan, J., Sun, Z. & Liu, S. NextPolish: a fast and efficient genome polishing tool for long-read assembly. *Bioinformatics* **36**, 2253–2255 (2020).
52. Vollger, M. R. et al. Improved assembly and variant detection of a haploid human genome using single-molecule, high-fidelity long reads. *Ann. Hum. Genet.* **84**, 125–140 (2020).
53. Wenger, A. M. et al. Highly-accurate long-read sequencing improves variant detection and assembly of a human genome. *Nat. Biotechnol.* **37**, 1155–1162 (2019).
This study introduces PacBio HiFi reads as a new data type and reveals the power of highly accurate (greater than 99%), long (greater than 10 kb) reads for *de novo* genome assembly and structural variant detection.
54. Vollger, M. R. et al. Long-read sequence and assembly of segmental duplications. *Nat. Methods* **16**, 88–94 (2019).
This article quantifies the extent to which segmental duplications remain unassembled in long-read genomes. Additionally, it describes a method to locally reconstruct segmental duplications by partitioning long-read sequence data using paralogous sequence variant graphs and locally assembling them.
55. Nurk, S. et al. HiCanu: accurate assembly of segmental duplications and allelic variants from high-fidelity long reads. Preprint at *bioRxiv* <https://doi.org/10.1101/2020.03.14.992248> (2020).
56. Miao, H. et al. Long-read sequencing identified a causal structural variant in an exome-negative case and enabled preimplantation genetic diagnosis. *Hereditas* **155**, 32 (2018).
57. Wick, R. R., Judd, L. M. & Holt, K. E. Performance of neural network basecalling tools for Oxford Nanopore sequencing. *Genome Biol.* **20**, 129 (2019).
58. Li, C. et al. INC-Seq: accurate single molecule reads using nanopore sequencing. *Gigascience* **5**, 34 (2016).
59. Wilson, B. D., Eisenstein, M. & Soh, H. T. High-fidelity nanopore sequencing of ultra-short DNA targets. *Anal. Chem.* **91**, 6783–6789 (2019).
60. Oxford Nanopore. 1D squared kit available in the store: boost accuracy, simple prep. *Oxford Nanopore Technologies* <http://nanoporetech.com/about-us/news/1d-squared-kit-available-store-boost-accuracy-simple-prep> (2017).
61. Lewandowski, K. et al. Metagenomic nanopore sequencing of influenza virus direct from clinical respiratory samples. *J. Clin. Microbiol.* **58**, e00963-19 (2019).
62. Charalampous, T. et al. Nanopore metagenomics enables rapid clinical diagnosis of bacterial lower respiratory infection. *Nat. Biotechnol.* **37**, 783–792 (2019).
63. Quick, J. et al. Real-time, portable genome sequencing for Ebola surveillance. *Nature* **530**, 228–232 (2016).
64. Pendleton, M. et al. Assembly and diploid architecture of an individual human genome via single-molecule technologies. *Nat. Methods* **12**, 780–786 (2015).
65. Okubo, M. et al. GGC repeat expansion of NOTCH2NL in adult patients with leukoencephalopathy. *Ann. Neurol.* **86**, 962–968 (2019).
66. Sone, J. et al. Long-read sequencing identifies GGC repeat expansions in NOTCH2NL associated with neuronal intranuclear inclusion disease. *Nat. Genet.* **51**, 1215–1221 (2019).
The authors show that PacBio CLR and ONT long reads can detect structural variation in clinically relevant disease-risk genes, which were previously missed with short-read whole-exome and whole-genome sequencing.
67. Stefansson, H. et al. Large recurrent microdeletions associated with schizophrenia. *Nature* **455**, 232–236 (2008).
68. Sharp, A. J. et al. Discovery of previously unidentified genomic disorders from the duplication architecture of the human genome. *Nat. Genet.* **38**, 1038–1042 (2006).
69. Hsieh, P. et al. Adaptive archaic introgression of copy number variants and the discovery of previously unknown human genes. *Science* **366**, eaax2083 (2019).
The authors describe large structural variants, originating in Neanderthals or Denisovans, that show signs of adaptation and positive selection in the Melanesian population. In particular, they use long reads to assemble a 386-kb duplication polymorphism that is present in 79% of Melanesians but generally absent from other populations, demonstrating the importance of developing new human reference genomes.
70. Shi, L. et al. Long-read sequencing and *de novo* assembly of a Chinese genome. *Nat. Commun.* **7**, 12065 (2016).
71. Seo, J.-S. et al. *De novo* assembly and phasing of a Korean human genome. *Nature* **538**, 243–247 (2016).
72. International Human Genome Project Consortium. Initial sequencing and analysis of the human genome. *Nature* **409**, 860–921 (2001).
73. Koren, S. et al. Canu: scalable and accurate long-read assembly via adaptive k-mer weighting and repeat separation. *Genome Res.* **27**, 722–736 (2017).
74. Chin, C.-S. & Khalak, A. Human genome assembly in 100 minutes. Preprint at *bioRxiv* <https://doi.org/10.1101/705616> (2019).
This article describes a unique and fast genome assembly algorithm called Peregrine that uses PacBio HiFi data. This long-read assembler is able to assemble a human genome in less than 100 minutes or ~ 30 CPU hours.
75. Chin, C.-S. et al. Phased diploid genome assembly with single-molecule real-time sequencing. *Nat. Methods* **13**, 1050–1054 (2016).
76. Kolmogorov, M., Yuan, J., Lin, Y. & Pevzner, P. A. Assembly of long, error-prone reads using repeat graphs. *Nat. Biotechnol.* **37**, 540–546 (2019).
77. Ruan, J. & Li, H. Fast and accurate long-read assembly with wtdbg2. *Nat. Methods* **17**, 155–158 (2020).
78. Steinberg, K. M. et al. High-quality assembly an individual of Yoruban descent. Preprint at *bioRxiv* <https://doi.org/10.1101/067447> (2016).
79. Oliver, J. S. et al. High-definition electronic genome maps from single molecule data. Preprint at *bioRxiv* <https://doi.org/10.1101/139840> (2017).
80. Udall, J. A. & Dawe, R. K. Is it ordered correctly? Validating genome assemblies by optical mapping. *Plant Cell* **30**, 7–14 (2018).
81. Ameer, A. et al. *De novo* assembly of two Swedish genomes reveals missing segments from the human GRCh38 reference and improves variant calling of population-scale sequencing data. *Genes* **9**, 486 (2018).
82. Li, H. Aligning sequence reads, clone sequences and assembly contigs with BWA-MEM. Preprint at *arXiv* <https://arxiv.org/abs/1303.3997> (2013).
83. Watson, M. & Warr, A. Errors in long-read assemblies can critically affect protein prediction. *Nat. Biotechnol.* **37**, 124–126 (2019).
84. Koren, S., Philipp, A. M., Simpson, J. T., Loman, N. J. & Loose, M. Reply to ‘Errors in long-read assemblies can critically affect protein prediction’. *Nat. Biotechnol.* **37**, 127–128 (2019).
85. Loman, N. J., Quick, J. & Simpson, J. T. A complete bacterial genome assembled *de novo* using only nanopore sequencing data. *Nat. Methods* **12**, 733–735 (2015).

86. Simpson, J. T. et al. Detecting DNA cytosine methylation using nanopore sequencing. *Nat. Methods* **14**, 407–410 (2017).
The authors report a method to detect methylated cytosines in raw ONT reads based on characteristic signal disruptions in ONT data using the computational tool Nanopolish. This tool is used to map methylation within the centromere for the first time.
87. Koren, S. et al. *De novo* assembly of haplotype-resolved genomes with trio binning. *Nat. Biotechnol.* **36**, 1174–1182 (2018).
The authors demonstrate a method to phase haplotypes for de novo genome assembly known as trio binning in which reads from the parents are used to identify and partition reads from the child into haplotypes before sequence assembly.
88. Porubský, D. et al. Direct chromosome-length haplotyping by single-cell sequencing. *Genome Res.* **26**, 1565–1574 (2016).
89. Patterson, M. et al. WhatsHap: weighted haplotype assembly for future-generation sequencing reads. *J. Computational Biol.* **22**, 498–509 (2015).
90. Kronenberg, Z. N. et al. Extended haplotype phasing of *de novo* genome assemblies with FALCON-Phase. Preprint at *bioRxiv* <https://doi.org/10.1101/327064> (2019).
91. Porubsky, D. et al. A fully phased accurate assembly of an individual human genome. Preprint at *bioRxiv* <https://doi.org/10.1101/855049> (2019).
92. Eichler, E. E. Recent duplication, domain accretion and the dynamic mutation of the human genome. *Trends Genet.* **17**, 661–669 (2001).
93. Rodriguez, O. L., Ritz, A., Sharp, A. J. & Bashir, A. MsPAC: A tool for haplotype-phased structural variant detection. *Bioinformatics* **36**, 922–924 (2019).
94. Bzikadze, A. V. & Pevzner, P. A. centroFlye: assembling centromeres with long error-prone reads. Preprint at *bioRxiv* <https://doi.org/10.1101/772103> (2019).
95. Ebbert, M. T. W. et al. Systematic analysis of dark and camouflaged genes reveals disease-relevant genes hiding in plain sight. *Genome Biol.* **20**, 97 (2019).
96. Feng, Z. et al. Detecting DNA modifications from SMRT sequencing data by modeling sequence context dependence of polymerase kinetic. *PLoS Comput. Biol.* **9**, e1002935 (2013).
97. Sedlazeck, F. J. et al. Accurate detection of complex structural variations using single molecule sequencing. *Nat. Methods* **15**, 461–468 (2018).
98. Chaisson, M. J. & Tesler, G. Mapping single molecule sequencing reads using basic local alignment with successive refinement (BLASR): application and theory. *BMC Bioinformatics* **13**, 238 (2012).
99. Li, H. Minimap2: pairwise alignment for nucleotide sequences. *Bioinformatics* **34**, 3094–3100 (2018).
100. Berlin, K. et al. Assembling large genomes with single-molecule sequencing and locality-sensitive hashing. *Nat. Biotechnol.* **33**, 623–630 (2015).
101. Mizuguchi, T. et al. A 12-kb structural variation in progressive myoclonic epilepsy was newly identified by long-read whole-genome sequencing. *J. Hum. Genet.* **64**, 359–368 (2019).
102. Merker, J. D. et al. Long-read genome sequencing identifies causal structural variation in a Mendelian disease. *Genet. Med.* **20**, 159–163 (2018).
103. Zeng, S. et al. Long-read sequencing identified intronic repeat expansions in SAMD12 from Chinese pedigrees affected with familial cortical myoclonic tremor with epilepsy. *J. Med. Genet.* **56**, 265–270 (2019).
104. Reiner, J. et al. Cytogenomic identification and long-read single molecule real-time (SMRT) sequencing of a Bardet–Biedl syndrome 9 (BBS9) deletion. *NPJ Genom. Med.* **3**, 3 (2018).
105. Sato, N. et al. Spinocerebellar ataxia type 31 is associated with ‘inserted’ penta-nucleotide repeats containing (TGGAA)*n*. *Am. J. Hum. Genet.* **85**, 544–557 (2009).
106. Dutta, U. R. et al. Breakpoint mapping of a novel *de novo* translocation t(X;20)(q11.1;p13) by positional cloning and long read sequencing. *Genomics* **111**, 1108–1114 (2019).
107. de Jong, L. C. et al. Nanopore sequencing of full-length BRCA1 mRNA transcripts reveals co-occurrence of known exon skipping events. *Breast Cancer Res.* **19**, 127 (2017).
108. Wenzel, A. et al. Single molecule real time sequencing in ADTKD-MUC1 allows complete assembly of the VNTR and exact positioning of causative mutations. *Sci. Rep.* **8**, 4170 (2018).
109. Ishiura, H. et al. Noncoding CGG repeat expansions in neuronal intranuclear inclusion disease, oculopharyngodistal myopathy and an overlapping disease. *Nat. Genet.* **51**, 1222–1232 (2019).
110. Aneichyk, T. et al. Dissecting the causal mechanism of X-linked dystonia-parkinsonism by integrating genome and transcriptome assembly. *Cell* **172**, 897–909.e21 (2018).
111. Song, J. H. T., Lowe, C. B. & Kingsley, D. M. Characterization of a human-specific tandem repeat associated with bipolar disorder and schizophrenia. *Am. J. Hum. Genet.* **103**, 421–430 (2018).
112. Carvalho, C. M. B. et al. Interchromosomal template-switching as a novel molecular mechanism for imprinting perturbations associated with Temple syndrome. *Genome Med.* **11**, 25 (2019).
113. Giesselmann, P. et al. Analysis of short tandem repeat expansions and their methylation state with nanopore sequencing. *Nat. Biotechnol.* **37**, 1478–1481 (2019).
114. Sulovari, A. et al. Human-specific tandem repeat expansion and differential gene expression during primate evolution. *Proc. Natl Acad. Sci. USA* **116**, 23243–23253 (2019).
115. Lei, X. X. et al. TTCA repeat expansion causes familial cortical myoclonic tremor with epilepsy. *Eur. J. Neurol.* **26**, 513–518 (2019).
116. Fiddes, I. T. et al. Human-specific NOTCH2NL genes affect Notch signaling and cortical neurogenesis. *Cell* **173**, 1356–1369.e22 (2018).
117. Suzuki, I. K. et al. Human-specific NOTCH2NL genes expand cortical neurogenesis through Delta/Notch regulation. *Cell* **173**, 1370–1384.e16 (2018).
118. Mefford, H. C. et al. Recurrent rearrangements of chromosome 1q21.1 and variable pediatric phenotypes. *N. Engl. J. Med.* **359**, 1685–1699 (2008).
119. Brunetti-Pierri, N. et al. Recurrent reciprocal 1q21.1 deletions and duplications associated with microcephaly or macrocephaly and developmental and behavioral abnormalities. *Nat. Genet.* **40**, 1466–1471 (2008).
120. He, Y. et al. Long-read assembly of the Chinese rhesus macaque genome and identification of ape-specific structural variants. *Nat. Commun.* **10**, 4233 (2019).
121. National Human Genome Research Institute. NHGRI funds centers for advancing the reference sequence of the human genome. *Genome.gov* <https://www.genome.gov/news/news-release/NIH-funds-centers-for-advancing-sequence-of-human-genome-reference> (2019).
122. Garalde, D. R. et al. Highly parallel direct RNA sequencing on an array of nanopores. *Nat. Methods* **15**, 201–206 (2018).
The authors describe a method to sequence full-length native RNA molecules with ONT sequencing technologies, simplifying the process by removing the steps to convert RNA into cDNA before sequencing.
123. Workman, R. E. et al. Nanopore native RNA sequencing of a human poly(A) transcriptome. *Nat. Methods* **16**, 1297–1305 (2019).
124. Soneson, C. et al. A comprehensive examination of Nanopore native RNA sequencing for characterization of complex transcriptomes. *Nat. Commun.* **10**, 3359 (2019).
125. Flusberg, B. A. et al. Direct detection of DNA methylation during single-molecule, real-time sequencing. *Nat. Methods* **7**, 461–465 (2010).
126. Vilfan, I. D. et al. Analysis of RNA base modification and structural rearrangement by single-molecule real-time detection of reverse transcription. *J. Nanobiotechnol.* **11**, 8 (2013).
127. Rand, A. C. et al. Mapping DNA methylation with high-throughput nanopore sequencing. *Nat. Methods* **14**, 411–413 (2017).
128. Sharon, D., Tilgner, H., Grubert, F. & Snyder, M. A single-molecule long-read survey of the human transcriptome. *Nat. Biotechnol.* **31**, 1009–1014 (2013).
129. Au, K. F. et al. Characterization of the human ESC transcriptome by hybrid sequencing. *Proc. Natl Acad. Sci. USA* **110**, E4821–E4830 (2013).
This article shows that full-length mRNA transcripts can be sequenced from end to end to identify novel gene isoforms using the PacBio Iso-Seq method. This article also provides a catalogue of the poly(A) transcriptome in human embryonic stem cells using a combination of Iso-Seq and short-read sequencing data.
130. Byrne, A. et al. Nanopore long-read RNAseq reveals widespread transcriptional variation among the surface receptors of individual B cells. *Nat. Commun.* **8**, 16027 (2017).
131. Oikonomopoulos, S., Wang, Y. C., Djambazian, H., Badescu, D. & Ragoussis, J. Benchmarking of the Oxford Nanopore MinION sequencing for quantitative and qualitative assessment of cDNA populations. *Sci. Rep.* **6**, 31602 (2016).
132. Dougherty, M. L. et al. Transcriptional fates of human-specific segmental duplications in brain. *Genome Res.* **28**, 1566–1576 (2018).
133. Volden, R. et al. Improving nanopore read accuracy with the R2C2 method enables the sequencing of highly multiplexed full-length single-cell cDNA. *Proc. Natl Acad. Sci. USA* **115**, 9726–9731 (2018).
134. Aird, D. et al. Analyzing and minimizing PCR amplification bias in Illumina sequencing libraries. *Genome Biol.* **12**, R18 (2011).
135. Clark, M. B. et al. Long-read sequencing reveals the complex splicing profile of the psychiatric risk gene CACNA1C in human brain. *Mol Psychiatry* **25**, 37–47 (2020).
136. Tang, A. D. et al. Full-length transcript characterization of SF3B1 mutation in chronic lymphocytic leukemia reveals downregulation of retained introns. *Nat. Commun.* **11**, 1438 (2020).
137. Clark, T. A. et al. Characterization of DNA methyltransferase specificities using single-molecule, real-time DNA sequencing. *Nucleic Acids Res.* **40**, e29 (2012).
138. Huang, Y. et al. The behaviour of 5-hydroxymethyl-cytosine in bisulfite sequencing. *PLoS One* **5**, e8888 (2010).
139. Pacific Biosciences. Detecting DNA base modifications using single molecule, real-time sequencing. *PacBio* https://www.pacb.com/wp-content/uploads/2015/09/WP_Detecting_DNA_Base_Modifications_Using_SMRT_Sequencing.pdf (2015).
140. Frommer, M. et al. A genomic sequencing protocol that yields a positive display of 5-methylcytosine residues in individual DNA strands. *Proc. Natl Acad. Sci. USA* **89**, 1827–1831 (1992).
141. An, N., Fleming, A. M., White, H. S. & Burrows, C. J. Nanopore detection of 8-oxoguanine in the human telomere repeat sequence. *ACS Nano* **9**, 4296–4307 (2015).
142. Liu, H. et al. Accurate detection of m⁶A RNA modifications in native RNA sequences. *Nat. Commun.* **10**, 4079 (2019).
143. Leger, A. et al. RNA modifications detection by comparative Nanopore direct RNA sequencing. Preprint at *bioRxiv* <https://doi.org/10.1101/843136> (2019).
144. Lorenz, D. A., Sathe, S., Einstein, J. M. & Yeo, G. W. Direct RNA sequencing enables m⁶A detection in endogenous transcript isoforms at base specific resolution. *RNA* <https://doi.org/10.1261/rna.072785.119> (2019).
145. Li, Y. & Tollefsbol, T. O. DNA methylation detection: bisulfite genomic sequencing analysis. *Methods Mol. Biol.* **791**, 11–21 (2011).
146. Schaefer, M., Pollex, T., Hanna, K. & Lyko, F. RNA cytosine methylation analysis by bisulfite sequencing. *Nucleic Acids Res.* **37**, e12 (2009).
147. Levanon, E. Y. et al. Systematic identification of abundant A-to-I editing sites in the human transcriptome. *Nat. Biotechnol.* **22**, 1001–1005 (2004).
148. Incarnato, D. et al. High-throughput single-base resolution mapping of RNA 2'-O-methylated residues. *Nucleic Acids Res.* **45**, 1433–1441 (2017).
149. Bakin, A. V. & Ofengand, J. Mapping of pseudouridine residues in RNA to nucleotide resolution. *Methods Mol. Biol.* **77**, 297–309 (1998).
150. Tsai, Y.-C. et al. Amplification-free, CRISPR-Cas9 targeted enrichment and SMRT sequencing of repeat-expansion disease causative genomic regions. Preprint at *bioRxiv* <https://doi.org/10.1101/203919> (2017).
151. Hafford-Tear, N. J. et al. CRISPR/Cas9-targeted enrichment and long-read sequencing of the Fuchs endothelial corneal dystrophy-associated TCF4 triplet repeat. *Genet. Med.* **21**, 2092–2102 (2019).
152. Suzuki, Y. et al. Agln: measuring the landscape of CpG methylation of individual repetitive elements. *Bioinformatics* **32**, 2911–2919 (2016).
153. Ni, P. et al. DeepSignal: detecting DNA methylation state from Nanopore sequencing reads using deep-learning. *Bioinformatics* **35**, 4586–4595 (2019).
154. McIntyre, A. B. R. et al. Single-molecule sequencing detection of N⁶-methyladenine in microbial reference materials. *Nat. Commun.* **10**, 579 (2019).
155. Liu, Q. et al. Detection of DNA base modifications by deep recurrent neural network on Oxford Nanopore sequencing data. *Nat. Commun.* **10**, 2449 (2019).

156. Stoiber, M. et al. De novo identification of DNA modifications enabled by genome-guided nanopore signal processing. Preprint at *bioRxiv* <https://doi.org/10.1101/094672> (2017).
157. Lee, I. et al. Simultaneous profiling of chromatin accessibility and methylation on human cell lines with nanopore sequencing. Preprint at *bioRxiv* <https://doi.org/10.1101/504993> (2019).
158. Beyter, D. et al. Long read sequencing of 1,817 Icelanders provides insight into the role of structural variants in human disease. Preprint at *bioRxiv* <https://doi.org/10.1101/848366> (2019).
159. Garrison, E. et al. Variation graph toolkit improves read mapping by representing genetic variation in the reference. *Nat. Biotechnol.* **36**, 875–879 (2018).
160. Schneider, V. A. et al. Evaluation of GRCh38 and de novo haploid genome assemblies demonstrates the enduring quality of the reference assembly. *Genome Res.* **27**, 849–864 (2017).
161. Li, R. et al. Building the sequence map of the human pan-genome. *Nat. Biotechnol.* **28**, 57–63 (2010).
162. Gnerre, S. et al. High-quality draft assemblies of mammalian genomes from massively parallel sequence data. *Proc. Natl Acad. Sci. USA* **108**, 1513–1518 (2011).
163. Sanders, A. D., Falconer, E., Hills, M., Spierings, D. C. J. & Lansdorp, P. M. Single-cell template strand sequencing by Strand-seq enables the characterization of individual homologs. *Nat. Protoc.* **12**, 1151–1176 (2017).
164. Sanders, A. D. et al. Single-cell analysis of structural variations and complex rearrangements with tri-channel processing. *Nat. Biotechnol.* **38**, 343–354 (2020).
165. Porubsky, D. et al. Dense and accurate whole-chromosome haplotyping of individual genomes. *Nat. Commun.* **8**, 1293 (2017).
166. Wu, J. K. et al. Thrombocytopenia-absent radius syndrome: background, pathophysiology, epidemiology. *Medscape* <https://reference.medscape.com/article/959262-overview> (2019).
167. Rosenfeld, J. A. et al. Proximal microdeletions and microduplications of 1q21.1 contribute to variable abnormal phenotypes. *Eur. J. Hum. Genet.* **20**, 754–761 (2012).

Acknowledgements

The authors thank M. J. Chaisson and D. Porubsky for assistance with the figures, K. Munson for technical assistance and commentarial insight and T. Brown for assistance in editing the manuscript. This work was supported, in part, by grants from the US National Institutes of Health (HG010169 to E.E.E.) and the US National Institute of General Medical Sciences (1F32GM134558-01 to G.A.L.). M.R.V. was supported by a US National Library of Medicine Big Data Training Grant for Genomics and Neuroscience (5T32LM012419-04). E.E.E. is an investigator of the Howard Hughes Medical Institute.

Author contributions

The authors contributed equally to all aspects of the article.

Competing interests

E.E.E. is on the scientific advisory board of DNAnexus Inc.

Peer review information

Nature Reviews Genetics thanks M. Schatz and the other, anonymous, reviewer(s) for their contribution to the peer review of this work.

Publisher's note

Springer Nature remains neutral with regard to jurisdictional claims in published maps and institutional affiliations.

Supplementary information

Supplementary information is available for this paper at <https://doi.org/10.1038/s41576-020-0236-x>.

RELATED LINKS

All of Us: <https://allofus.nih.gov/>

Arrow: <https://github.com/PacificBiosciences/GenomicConsensus>

Loman Labs: <https://lab.loman.net/2017/03/09/ultrareads-for-nanopore/>

Medaka: <https://github.com/nanoporetech/medaka>

Nanopolish: <https://github.com/jts/nanopolish>

Pacific Biosciences: does speed impact quality and yield?:

<https://github.com/PacificBiosciences/ccs#does-speed-impact-quality-and-yield>

© Springer Nature Limited 2020